Journal of Sedimentary Research

Journal of Sedimentary Research, 2022, v. 92, 1186–1206
Current Ripples
DOI: 10.2110/jsr.2022.013

AN EOLIAN DUST ORIGIN FOR CLASTIC FINES OF DEVONO-MISSISSIPPIAN MUDROCKS OF THE GREATER NORTH AMERICAN MIDCONTINENT

AUSTIN J. McGLANNAN,[1] ALICIA BONAR,[1] LILY PFEIFER,[1] SEBASTIAN STEINIG,[2] PAUL VALDES,[2] STEVEN ADAMS,[1] DAVID DUARTE,[1] BENMADI MILAD,[1] ANDREW CULLEN,[3] AND GERILYN S. SOREGHAN[1]

[1]*University of Oklahoma, School of Geosciences, Norman, Oklahoma 73019, U.S.A.*
[2]*University of Bristol, School of Geographical Sciences, Bristol, U.K.*
[3]*Independent Geoscientist, Norman, Oklahoma 73072, U.S.A.*

ABSTRACT: **Upper Devonian and Lower–Middle Mississippian strata of the North American midcontinent are ubiquitously fine-grained and silt-rich, comprising both so-called shale as well as argillaceous limestone (or calcareous siltstone) that accumulated in the Laurentian epeiric sea. Although long recognized as recording marine deposition, the origin and transport of the fine-grained siliciclastic material in these units remains enigmatic because they do not connect to any proximal deltaic feeder systems. Here, we present new data on grain size, whole-rock geochemistry, mineralogy, and U-Pb detrital-zircon geochronology from units across Oklahoma; we then integrate these data with models of surface wind circulation, refined paleogeographic reconstructions, and correlations from the greater midcontinent to test the hypothesis that wind transported the siliciclastic fraction to the marine system. The exclusively very fine silt to very fine sand grain size, clear detrital origin, widespread distribution over large regions of the epeiric sea, Appalachian sources, and paleogeographic setting in the subtropical arid belt far-removed from contemporaneous deltaic feeder systems are most consistent with eolian transport of dust lofted from subaerial delta plains of the greater Appalachian orogen and incorporated into subaqueous depositional systems. Delivery of dust that was minimally chemically weathered to Devono-Mississippian epeiric seas likely provided essential nutrients that stimulated organic productivity in these commonly organic-rich units.**

INTRODUCTION

Siltstone, argillaceous siltstone, silty carbonate, siliciclastic mudstone, shale, and chert are common lithofacies in the upper Devonian–Middle Mississippian strata in basins of the North American midcontinent that accumulated in epeiric seas of the southern Laurentian craton (Fig. 1, 2; Lowe 1976; Lane and De Keyser 1980; Gutschick and Sandberg 1983; Over 1990; Schwartzapfel 1990; Turner et al. 2015; Schieber 2016; Kondas et al. 2018; Godwin et al. 2019; Mazzullo et al. 2019; Miller et al. 2019b; Milad et al. 2020; Price et al. 2020). These strata are commonly organic-rich, and have attracted interest primarily as petroleum source rocks and unconventional reservoirs (Barrows and Cluff 1984; Smith and Bustin 1998; Smith and Bustin 2000; Slatt and O'Brien 2011; Angulo and Buatois 2012; Higley 2013; Wang and Philp 2019), but they also provide insights on climate, tectonics, and carbon sequestration of the time. The range of explanations for deposition of the siliciclastic fraction includes: 1) suspension settling (Kirkland et al. 1992; Smith and Bustin 1998), 2) a combination of suspension settling, density currents, and gravity flows (e.g., Wright and Friedrichs 2006; Loucks and Ruppel 2007; Macquaker et al. 2010; Milad et al. 2020; Price et al. 2020), and 3) wind- or tide-induced subaqueous currents that remobilized muds across ancient epeiric seas (Schieber 2016). Although all accept that these strata ultimately accumulated in marine environments, the provenance, generation, and transport of the significant volume of uniformly fine-grained siliciclastic material remain enigmatic and unresolved.

To better constrain the origin and transport of the siliciclastic fraction in these units, this work integrates new data from Upper Devonian and Lower–Middle Mississippian siltstone, mudrock, and argillaceous carbonate units across Oklahoma with compilations of coeval systems of the greater midcontinent region (Fig. 2). We use these data to test the hypothesis of eolian delivery to the marine environment for the vast volume of this material. An eolian-dust origin explains otherwise perplexing attributes of these units and has significant implications for interpretation of organic productivity in these and analogous systems.

GEOLOGICAL BACKGROUND, PALEOGEOGRAPHY, AND PALEOCLIMATE

The Anadarko Basin was initially part of the Oklahoma Basin (Johnson et al. 1988) which originated in the Early Cambrian in response to thermal subsidence associated with development of the Southern Oklahoma Aulacogen (Wickham 1978; Dalziel 1991; Meert and Torsvik 2003). Cambro-Ordovician carbonate strata accumulated in the axis of the failed rift (Perry 1989) as a broad epicontinental shelf developed on the flanks (Johnson et al. 1989). Carbonate and, subordinately, siliciclastic mudstone sedimentation continued through the Devono-Mississippian (e.g., Hunton Limestone, Woodford Shale, Sycamore Limestone, Caney Shale), a time of relative tectonic quiescence in this part of the Anadarko Basin and greater midcontinent region, before the tectonic disruptions of the Ouachita and Ancestral Rocky Mountains orogenies (Feinstein 1981; Johnson et al. 1988, 1989). Closure of the Rheic Ocean and associated contractional

Published Online: December 2022

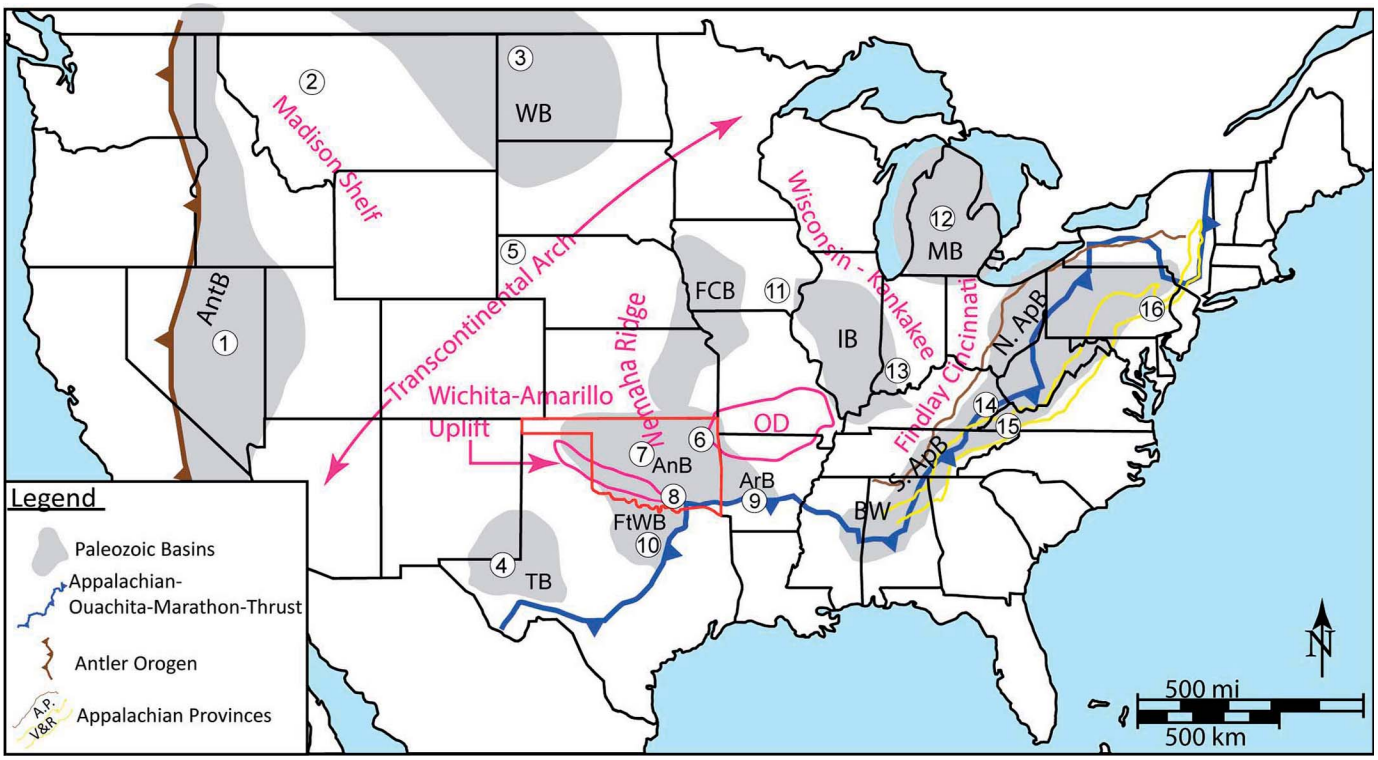

FIG. 1.—Major basins (gray shading), domes, and arches (red lines and text) of the U.S. for the Devono-Mississippian. Abbreviations are as follows: AnB, Anadarko Basin; AntB, Antler Basin, ArB, Arkoma Basin; BWB, Black Warrior Basin; FCB, Forest City Basin; FtWB, Fort Worth Basin; IB, Illinois Basin; MB, Michigan Basin; N. ApB, Northern Appalachian Basin; S. ApB, southern Appalachian Basin; TB, Tobosa Basin; WB, Williston Basin; OD, Ozark Dome. Numbers within circles correspond to locations of stratigraphic columns in Figure 2. Yellow polygon outlines the Appalachian Valley and Ridge Province (V&R). The edge of the brown polygon shows the western limit of the Appalachian Plateau Province (A.P.). Modified from Adams (1965), Gutschick and Sandberg (1983), Smith and Bustin (2000), Loucks and Ruppel (2007), Soeder et al. (2014), Ettensohn et al. (2019) and Thomas et al. (2020).

tectonics beginning in the latest Mississippian (Serpukhovian)–Early Pennsylvanian (Nance et al. 2010) ultimately produced the thin-skinned Ouachita fold-and-thrust belt and the associated Arkoma basin (Fig. 1). By Pennsylvanian time, a series of NW–SE-oriented basement-cored uplifts developed, termed the Ancestral Rocky Mountains, including the Wichita–Amarillo uplift and yoked Anadarko Basin of southwestern Oklahoma and northern Texas (Kluth and Coney 1981). The present configuration of the Anadarko Basin is a product of this compressional inversion of the earlier aulacogen along basement-involved reverse faults, and development of accommodation space along the mountain front (Johnson et al. 1989).

Beyond Oklahoma, Late Devonian orogenic events affected both the eastern and western margins of the craton, in the form of the Acadian–Neoacadian and Antler orogenies, respectively. The Acadian and Neoacadian orogenies produced a series of westward-prograding clastic wedges, the Catskill Delta complex during the Middle–Late Devonian and the Price–Pocono–Borden–Grainger delta complex during the Early–Middle Mississippian (Ettensohn and Woodrow 1985; Ettensohn 2004, 2008, 2022), whereas the Antler clastic wedge prograded eastward (Sandberg and Gutschick 1980; Johnson and Pendergast 1981) (Fig. 3). The Oklahoma Basin remained isolated and far removed from each of these clastic wedge complexes, ~ 1800 km from the Antler and ~ 1500 km from the Appalachian, throughout the Late Devonian to Middle Mississippian (Fig. 3). Note that we use North American stage names for the Mississippian, for consistency with the literature.

The eastern deltaic complexes are well exposed in outcrops and boreholes throughout the Appalachian Valley and Ridge and Appalachian Plateau provinces, and exhibit both marine and continental facies for nearly 1000 km along orogenic strike (Fig. 1). The Catskill Delta complex developed during the Middle to Late Devonian, transporting siliciclastics from the Acadian Orogen to marginal marine environments along the Appalachian foreland (Fig. 3). During the Famennian, this complex comprised an estimated four main delta systems, fed by low-gradient coastal rivers emanating from alluvial systems in the highlands—akin in scale to the Eocene and modern Texas–Louisiana coastal plain, or the northern Sumatran coast (Sevon 1985; Woodrow et al. 1985; Boswell and Donaldson 1988). Organic-rich black shales characterize the basinal facies of the Catskill Delta complex in the Appalachian foreland basin (Ettensohn and Woodrow 1985; Boswell and Donaldson 1988; Ettensohn 2008; Ettensohn et al. 2019).

Clastic-wedge deposition continued into the Early–Middle Mississippian (Kinderhookian–Osagean) in response to Neoacadian tectonism, such that the Appalachian foreland overfilled and deltaic deposition of the Borden and Grainger formations (Figs. 2, 3) prograded into the eastern and southeastern Illinois Basin (Ettensohn et al. 2022). Active denudation ceased in the Middle to Late Mississippian (Meramecian–middle Chesterian), resulting in extensive carbonate deposition in the Appalachian foreland (Greenbrier and Newman Limestones, Fig. 2; Ettensohn et al. 2022). Toward the eastern Appalachian foreland basin, carbonate strata intertongue with continental redbeds and eolianites throughout West Virginia, Virginia, and Maryland (Wynn and Read 2008; Ettensohn et al. 2022). Early development of the Mauch Chunk Delta began in eastern Pennsylvania in the Meramecian (Wynn and Read 2008; Ettensohn et al. 2022) (Fig. 3).

In the extensive cratonic region between the Acadian (east) and Antler (west) orogenic systems, broad epeiric seas, intracratonic basins, and emergent arches prevailed through the Late Devonian–Early Mississippian,

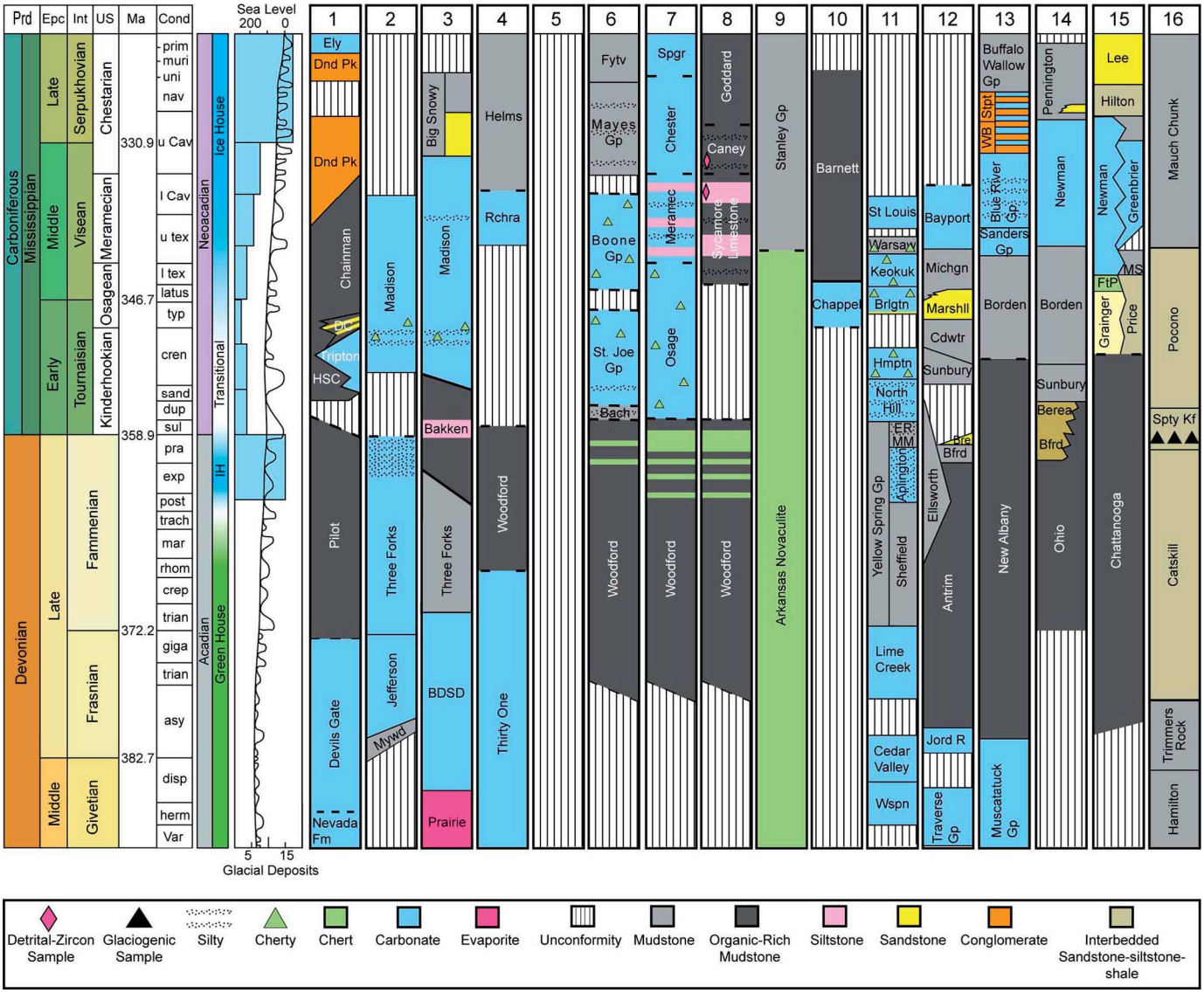

FIG. 2.—Regional stratigraphic correlation of Middle Devonian–Upper Mississippian units across the Laurentian craton from west (left) to east (right). Dark gray indicates units that are considered elevated in organic richness. Abbreviations on chronostratigraphic chart headings are as follows: Prd, Period; Epc, Epoch; Int, International Age; US, US Age; Cond, Conodonts. Numbered headings for each column correspond to locations denoted in Figure 1. Abbreviations for stratigraphy as follows: Dnd Pk, Diamond Peak; DC, Dale Canyon Formation; HSC, Homestead Canyon Formation; Mywd, Maywood; BDSD, Birdbear Fm, Duperow Fm, Souris River Fm, Dawson Bay Fm; Rchra, Rancheria Formation; Fytv, Fayetteville Shale; Bach, Bachelor Formation; Spgr, Springer Formation; Brlgtn, Burlington Limestone; Hmptn, Hampton Formation; ER, English River Formation; MM, Maple Mill Shale; Wspn, Wapsipinicon Formation; Michgn, Michigan Formation; Marshll, Marshall Sandstone; Cdwtr, Coldwater Shale; Bre, Berea Sandstone; Bfrd, Bedford Shale; Jord R, Jordan River Formation; Stpt, Stephensport Group; WB, West Baden Group; FtP, Ft. Payne; MS, MacCrady Shale. Spty Kf, Spechty Kopf Formation. See Supplemental File 2 for references used to construct this chart in addition to the abbreviations for conodont zonations.

with organic-rich mudstones, including the Chattanooga Shale, Ohio Shale, New Albany Shale, Antrim Shale, and Woodford Shale accumulating east of the Transcontinental Arch and correlative mudstones such as the Bakken Shale and Duvernay Shale accumulating west of the Transcontinental Arch (Figs. 2, 3). Carbonate-dominant systems with variably silty and cherty components prevailed through the Early–Middle Mississippian (e.g., the North Hill Limestone, Keokuk Limestone, St. Joe Group, Boone Group, Osage Limestone of northern Oklahoma, and Madison Limestone; Figs. 2, 3; Gutschick and Sandberg 1983, and others). By the Middle to Late Mississippian (Meramecian–late Chesterian), fine siliciclastic contents increased, with deposition of silty carbonates, marine siltstones, and silty organic-rich mudstones (e.g., Blue River Group, Warsaw Shale, Barnett Shale, Meramec and Sycamore formations, Caney Shale and Madison Limestone; Figs. 2, 3).

The midcontinent region ranged from southern subtropical latitudes (~ 15° S–30° S) in the Late Devonian to near-tropical latitudes (~ 15° S) by the Early–Middle Mississippian (e.g., Boucot et al. 2013; Domeier and Torsvik 2014; Scotese and Wright 2018) (Fig. 3). Paleoclimatic reconstructions document arid conditions in lowland regions throughout the midcontinent within these time intervals (Boucot et al. 2013) (Fig. 3). Additionally, a number of instances of ice-contact deposits document evidence for suspected icesheets and/or alpine and even tidewater glaciation within the central Appalachian orogenic system during the latest Devonian (approximately lower to middle *Siphonodella praesulcata* conodont zonation; LE, *Retispora lepidophyta–Indotriradites explanatus*

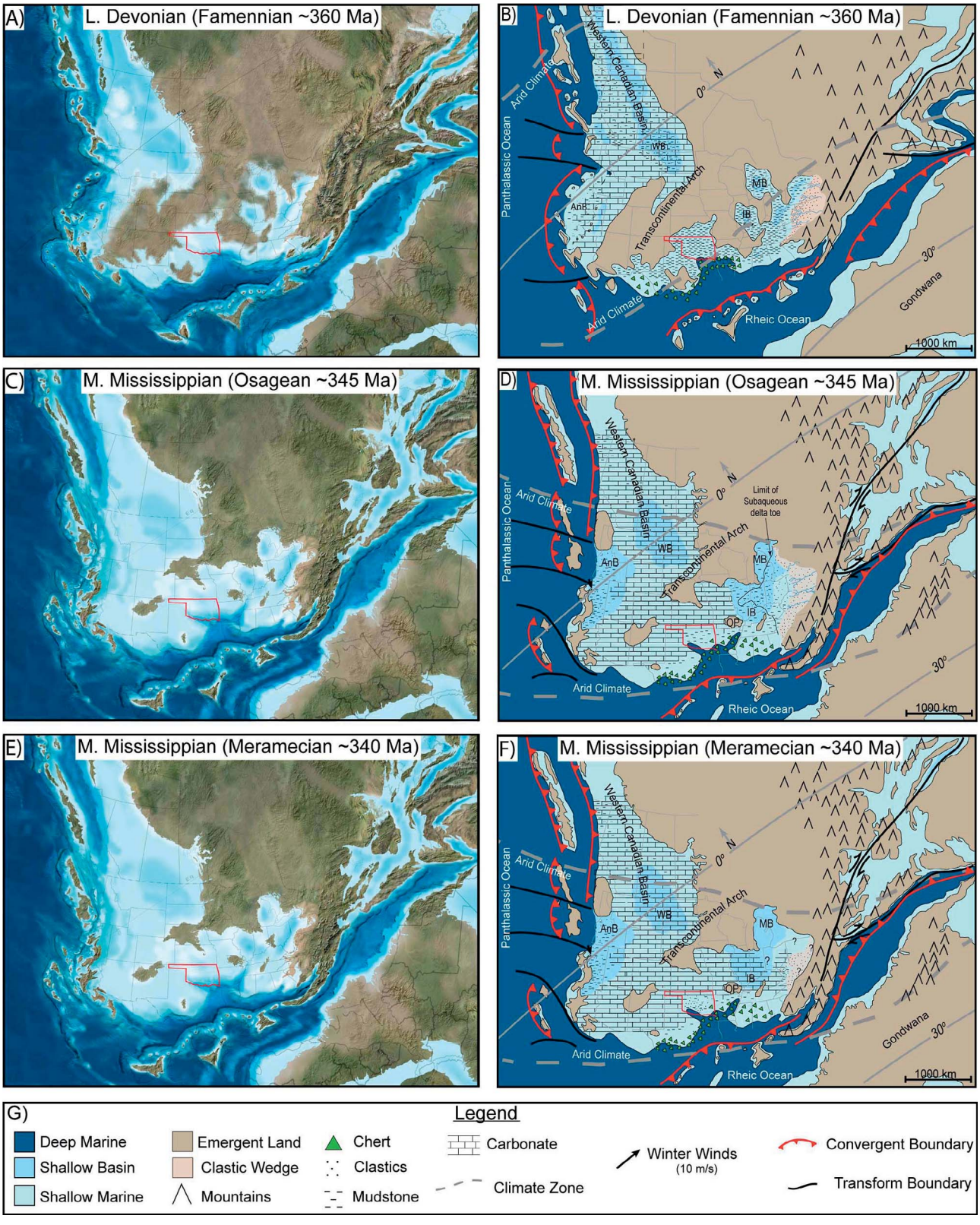

FIG. 3.—Late Devonian–Middle Mississippian paleogeographic reconstructions. Oklahoma is outlined in red for all panels. **A)** Paleogeography of the Late Devonian (~ 360 Ma, Famennian). **B)** Facies and tectonic map for the Famennian. The Catskill Delta complex is noted by a stippled beige polygon and fluvial systems (Boswell and Donaldson 1988). Midcontinent region and Oklahoma lie within the arid belt (Scotese and Wright 2018), whereas the Appalachians lie within a seasonally wet climate (Brezinski et al. 2009). **C)** Paleogeography of the Middle Mississippian (~ 345 Ma, Osagean). **D)** Middle Mississippian, Osagean, facies and tectonic paleogeographic map. The Price–Pocono Delta complex is noted by stippled beige polygon with sketched fluvial systems (Gutshick and Sandberg 1988; Ettensohn et al. 2022). Thin solid black line

to LN, *Retispora lepidophyta–Verrucosisporites nitidus* miospore zonation) (e.g., Spechty Kopf Formation, Isaacson et al. 2008; Brezinski et al. 2008, 2009, 2010; Lakin et al. 2016; Ettensohn et al. 2020a, 2020b) (Fig. 2).

Glaciation in the central Appalachians marks the apex of the late Devonian icehouse. Glaciation in Gondwanaland began in the late Famennian (approximately *Palmatolepis postera* conodont zonation; VCo, *Diducites versabilis–Grandispora cornuta* miospore zonation) and extended to the latest Famennian (Upper *Siphonodella praesulcata* conodont zonation; LN, *Retispora lepidophyta–Verrucosisporites nitidus* miospore zonation) (Fig. 2) (Caputo et al. 2008; Isaacson et al. 2008; Lakin et al. 2016). Additionally, minor evidence for Gondwanan glaciation exists for the Early and Middle Mississippian (Kinderhookian–Osagean and Meramecian–Chesterian) (Caputo et al. 2008; compilation in Soreghan et al. 2019).

MIDCONTINENT STRATIGRAPHY OF OKLAHOMA

In Table 1, we summarize the facies attributes and inferred depositional environments for Upper Devonian and Lower–Middle Mississippian strata of Oklahoma (Figs. 2, 4, 5). These units are well exposed and have been widely characterized in the Arbuckle Mountains (southern Oklahoma), the Ozark Plateau (northeastern Oklahoma), and the subsurface; correlatives occur throughout the greater midcontinent as demonstrated through hundreds of thousands of well penetrations (Craig et al. 1978; See Supplemental File 1).

METHODS

Paleogeographic Reconstructions

To place the study units (Fig. 4) in a broader context (Figs. 2, 3), we used the paleogeographic maps of Blakey (2013), North American Key Time Slices ©2013 Colorado Plateau Geosystems, Inc, as base maps, and appended these with major climate belts following Boucot et al. (2013) and Scotese and Wright (2018). The Correlation of Stratigraphic Units of North America (COSUNA) project charts (Ballard et al. 1983; Hills and Kottlowski 1983; Patchen et al. 1984a, 1984b; Bergstrom and Morey 1985; Hintze 1985; Shaver 1985; Adler 1986; Mankin 1987; Kent et al. 1988) provided the initial framework for age constraints and correlations, but all unit ages were updated with the most recent available data (Cohen et al. 2013) (See Supplemental File 2 for references).

Grain-Size Analysis

To assess the nature of and possible transport modes for the siliciclastic material in the target strata, we collected samples for particle-size analysis from seven outcrops and ten cores distributed throughout Oklahoma (Fig. 4; See Supplemental Files 2 and 3). While carbonate grains and iron oxides, as well as grain coatings, may constitute a minor fraction of the original detrital material, we specifically target the silicate mineral fraction (SMF) as a proxy for detrital grain size. Therefore, all organic, carbonate, and iron oxide components were removed using a sequential procedure following standard methods (cf. Sur et al. 2010a, 2010b; Jiang and Liu 2011; Sweet et al. 2013; Foster et al. 2014), as outlined briefly here.

Samples were gently crushed with a ceramic mortar and pestle to pea-size gravel to accelerate chemical reactions, then rinsed with distilled water and sieved at 250 μm to remove any fines generated during crushing. Samples were subsequently treated with 2N HCl (minimum 24 hours) for carbonate removal. To remove organic matter and oxidize pyrite, samples were combusted at 500 °C for ~ 12–20 hours. This does not affect the grain size of silicate minerals, since silicates do not begin to sinter until temperatures exceed 500 °C (Schomburg 1991; Rickard et al. 2016). Samples were then treated with sodium citrate–bicarbonate–dithionite (CBD) (Sur et al. 2010a; Rea and Janecek 1981) rinses until all iron oxides were removed.

Smear slides of residues were inspected using a polarizing reflected-light microscope under 10×, 20×, and 40× objectives to assess sample composition and ensure disaggregation, and check for the presence of remnant authigenic phases such as silicified microfossils (Fig. 6). If present, silicified microfossils were physically removed by sieving following visual inspection to determine appropriate sieve size needed to remove microfossils, microfossil fragments, and/or aggregates while retaining detrital material (See Supplemental Files 2 and 3 for additional information). Samples exhibiting a predominance of authigenic material were eliminated from analysis. Furthermore, both visual inspection and previous studies on these strata indicate no to minimal instances of quartz overgrowths (Shelley et al. 2019; Price et al. 2020; Milad et al. 2020; Duarte et al. 2021; Supplemental Files 3, 4), lending further confidence to the fidelity of subsequent particle-size analyses. Particle sizes of fully disaggregated samples were measured using a Malvern Mastersizer 3000 Laser Particle Size Analyzer (LPSA). Of 103 samples processed in this way, 82 disaggregated sufficiently to enable analysis by LPSA.

Geochemical Analysis

To address compositional characteristics of the silicate material in the Sycamore and Woodford Shale, nineteen ~ 5 g samples from the Arbuckle Uplift transect (Figs. 2, 4) were fragmented to gravel size and submerged in a 1N HCl for 24 hours to eliminate carbonate before whole-rock and trace-element geochemical analysis (acquired by ALS Geochemical). Remnant CaO values and high loss-on-ignition (LOI) necessitated application of the correction by Taylor and McClennan (1985) to interpret the silicate fraction. Data were analyzed (and biplots were created) using principal-components analysis (PCA) in R.

Detrital-Zircon Geochronology

To assess provenance of the siliciclastic material, three 10–20 kg samples from each of the Arbuckle Uplift units (Figs. 2, 4; Woodford Shale, Sycamore Limestone, and Caney Shale) were processed for zircon separation and analyzed for detrital-zircon geochronology at the University of Arizona (UA) LaserChron Center. Analyses were conducted using the Element 2 laser ablation–single collector–inductively coupled plasma–mass spectrometer (LA-SC-ICP-MS) following the analytical and data processing methods described in Pullen et al. (2018) and Gehrels and Pecha (2014). Insufficient yield from the Woodford Shale sample (despite

←

denotes the western limit of the subaqueous delta prograding from the Appalachians (Borden and Grainger Formations) (Ettensohn et al. 2022). **E)** Middle Mississippian (~ 340 Ma, Meramecian) paleogeography of Laurentia. **F)** Middle Mississippian, Meramecian, facies and tectonic paleogeographic map. Both Parts D and F show the midcontinent region within the subtropical arid climate belt, and far removed from shorelines. Widespread shallow water is present across the craton, including the Appalachian Basin, such as the Newman and Greenbrier limestones (Fig. 2) (Ettensohn et al. 2022). Stippled clastics in beige in the Appalachian Basin region of West Virginia, Virginia, Pennsylvania, denote late Meramecian coastal sands, silts, and eolian environments (Wynn and Read 2008; Ettensohn et al. 2022). Stipple and mudstone pattern sketched in Oklahoma (outlined in red), denote the deposition of the Meramec, Sycamore, and lower Caney Shale formations. Paleogeographic maps A, C, E are from Blakey (2013), North American Key Time Slices ©2013 Colorado Plateau Geosystems, Inc., and were used as base maps for Parts B, D, F. Paleoclimate boundaries are derived from Boucot et al. (2013) and Scotese and Wright (2018). See Supplemental File 2 for all references pertaining to construction of facies maps and tectonic maps.

TABLE 1.—*Devono-Mississippian mid-contient stratigraphy of Oklahoma. X, unconformity; Kinderh, Kinderhookian.*

Geographic Region	Period	Series/ Epoch	Age	Group/Formation	Lithologic Characteristics	Sedimentary Structures	Published Depositional Environments	Correlative Units	References
Arbuckle Uplift	Carboniferous Mississippian	Middle	Visean Chestarian	Caney Shale	Organic-rich mudstone. Thin limestone and siltstone beds. Phosphate and siderite nodules.	Massive. Faint laminae.	Marine. Not well resolved.	Meramec, Chester Limestone, Barnett Shale, Fayetteville Shale	Elias 1956; Schwartzapfel 1990; Kleehammer 1991; Andrews 2007; Miller et al. 2019a
			Meramecian	Sycamore–Meramec	Moderate to well sorted calcareous quartz siltstone containing peloids and bioclasts. Organic-rich argillacous units.	Hummocky and swaly cross-stratification. Partial Bouma sequences (Ta–Tb–Te). Scoured bases. Possible flute casts.	Initially interpreted as shallow-water carbonate. Subaqueous delta. Deep water fans.	Madison Limestone Group, St. Louis Limestone, middle parts of the Newman/Greenbrier Limestone.	Bennison 1956; Prestridge 1957; Cole 1988; Schwartzapfel 1990; Schwartzapfel and Holdsworth 1996; Miller and Cullen 2018; Miller et al. 2019a; Milad et al. 2020; Price et al. 2020
			Osagean	X	X	X	X	X	
		Early	Tournasian Kinderh						
	Devonian	Late	Famennian	Woodford Shale	Organic rich. Argillaceous layers interbedded with thin chert beds. Chert increases southward and upsection. Abundant phosphate nodules in upper section.	Laminated to massive and structureless argilaceous beds	Shelf, anoxic–euxinic marine	Chattanooga Shale, Ohio Shale, Antrim Shale, New Albany Shale, Arkansas Novaculite, Caballos Novaculite.	Over 1990; Turner et al. 2016; Connock et al. 2018; Kondas et al. 2018
			Frasnian						
Northeast Oklahoma	Carboniferous Mississippian	Middle	Visean Chestarian	Pryor Creek Formation	Calcareous siltstones and shales	Planar laminae. Low-angle cross-stratification. Bioturbation.	Carbonate ramp	Sycamore–Meramec and Caney Shale	Godwin and Puckette 2019; Godwin et al. 2019; Shelley et al. 2019
			Meramecian	Boone Group	Limestones, abundant chert, bioclastic glauconitic limestones	Cross-stratification	Inner to outer carbonate ramp	Borden Formation, Madison Limestone	Godwin et al. 2019; Mazzullo et al. 2019; Miller et al. 2019b
			Osagean	X	X	X	X	X	
		Early	Tournasian Kinderh	St. Joe Group	Micritic mudstones to crinoidal wackestone and grainstones. Variable siliciclastic silt and chert nodules.	Laminae. Tabular cross-stratification. Soft-sediment deformation.	Shallow marine. Tidal flats. Not well resolved.	pre-Welden Shale, Welden Limestone	Branch 1988; Mazzullo et al. 2013, 2019; Godwin et al. 2019
				Bachelor Formation	Silty glauconitic mudstone	Structureless	Nearshore marine	Posited to correlate with a thin green shale throughout Oklahoma informally named "Kinderhookian Shale"	Mazzullo et al. 2013, 2019
	Devonian	Late	Famennian	Woodford Shale	Organic rich. Argillaceous mudstone.	Laminated to massive and structureless argilaceous beds	Shelf, anoxic marine	Chattanooga Shale, Ohio Shale, Antrim Shale, New Albany Shale, Arkansas Novaculite, Caballos Novaculite.	Over 1990; Connock et al. 2018; this study
			Frasnian						

> 20 kg of processed material) precluded analysis. Best ages from the Sycamore Limestone and Caney Shale are reported as $^{206}Pb/^{207}Pb$ for ages greater than 900 Ma and $^{206}Pb/^{238}U$ for ages less than 900 Ma. These ages are displayed as normalized probability density plots using an Excel macro, provided by the UA LaserChron Center (Gehrels 2010). Analyses with > 10% discordance and 5% reverse discordance were eliminated before analysis.

General-Circulation Modeling

To address climatic attributes and potential atmospheric transport pathways, we reanalyzed results of a total of 12 coupled general-circulation-model (GCM) experiments of global climate from intervals spanning the Middle Devonian to the Late Mississippian. The simulations were performed with the HadCM3BL-M2.1aD atmosphere–ocean–vegetation model (Valdes et al. 2017) and are described in detail in Valdes et al. (2021). The model uses the same horizontal grid with a resolution of 3.75° × 2.5° in the atmosphere and ocean, with 19 and 20 unequally spaced vertical levels, respectively. The paleogeographies underlying the model simulations were derived from the PALEOMAP paleogeographic atlas (Scotese and Wright 2018). Current geographical coordinates of Oklahoma and the Appalachian clastic wedges were rotated using the PALEOMAP rotation model in the pyGplates software (Müller et al. 2018) to place these features within the appropriate paleogeographical positions. Locations for the Appalachian clastic wedges are from Ettensohn et al. (2019). Besides the model geography, the simulations differ only by a linearly increasing solar constant (0.8% per 100 Myr) and varying concentrations of atmospheric carbon dioxide. CO_2 levels for the selected simulations were derived from the Foster et al. (2017) curve and range from a peak of 1377 ppmv in the Middle Devonian to a minimum of 233 ppmv in the Middle

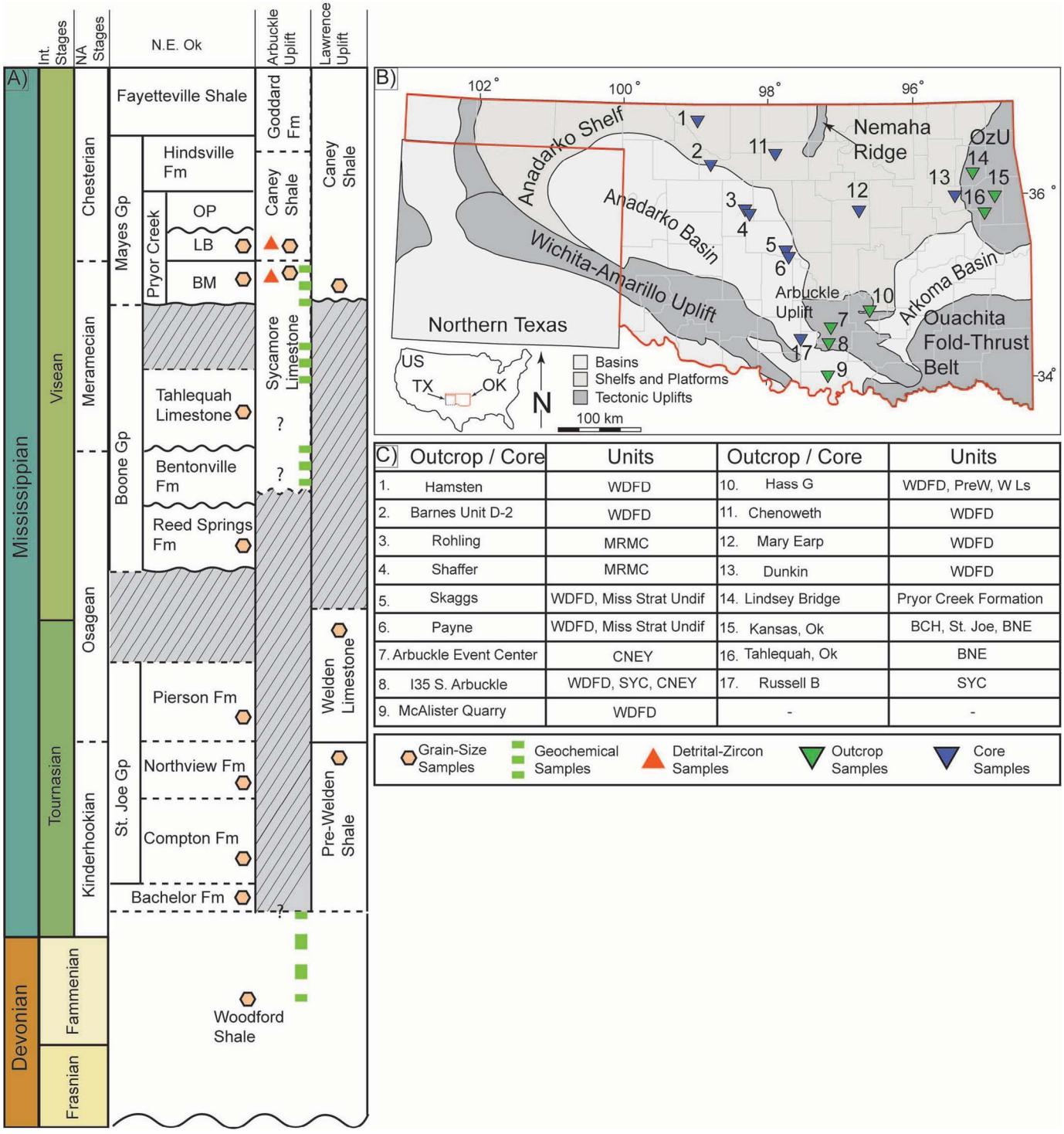

C) Outcrop / Core	Units	Outcrop / Core	Units
1. Hamsten	WDFD	10. Hass G	WDFD, PreW, W Ls
2. Barnes Unit D-2	WDFD	11. Chenoweth	WDFD
3. Rohling	MRMC	12. Mary Earp	WDFD
4. Shaffer	MRMC	13. Dunkin	WDFD
5. Skaggs	WDFD, Miss Strat Undif	14. Lindsey Bridge	Pryor Creek Formation
6. Payne	WDFD, Miss Strat Undif	15. Kansas, Ok	BCH, St. Joe, BNE
7. Arbuckle Event Center	CNEY	16. Tahlequah, Ok	BNE
8. I35 S. Arbuckle	WDFD, SYC, CNEY	17. Russell B	SYC
9. McAlister Quarry	WDFD	-	-

FIG. 4.—**A)** Local stratigraphic correlation chart between northeastern Oklahoma and southern Oklahoma. BM, Bayou Manard Member; LB, Lindsey Bridge Member; OP, Ordinance Plant Member. (Modified from Godwin et al. 2019, with additions from Branch 1988, Boardman et al. 2013, and Mazzullo et al. 2013, 2019). Note that stratigraphic column is not to scale in absolute time. **B)** Present-day physiographic map of Oklahoma's tectonic features. US, United States; OK, Oklahoma; TX, Texas; OzU, Ozark Uplift. Oklahoma is outlined in red. See Supplemental File 2 or 4 for exact coordinates for cores and outcrops. Base map modified from Campbell et al. (1988), Northcutt and Campbell (1995) and Miller et al. (2021). **C)** Legend for cores and outcrops plotted in Part B. WDFD, Woodford Shale; MRMC, Meramec; Miss Strat Undif, Mississippian Strata Undifferentiated; SYC, Sycamore Limestone; PreW, Pre-Welden Shale; W Ls, Welden Limestone; BCH Fm, Bachelor Formation; BNE Gp, Boone Group.

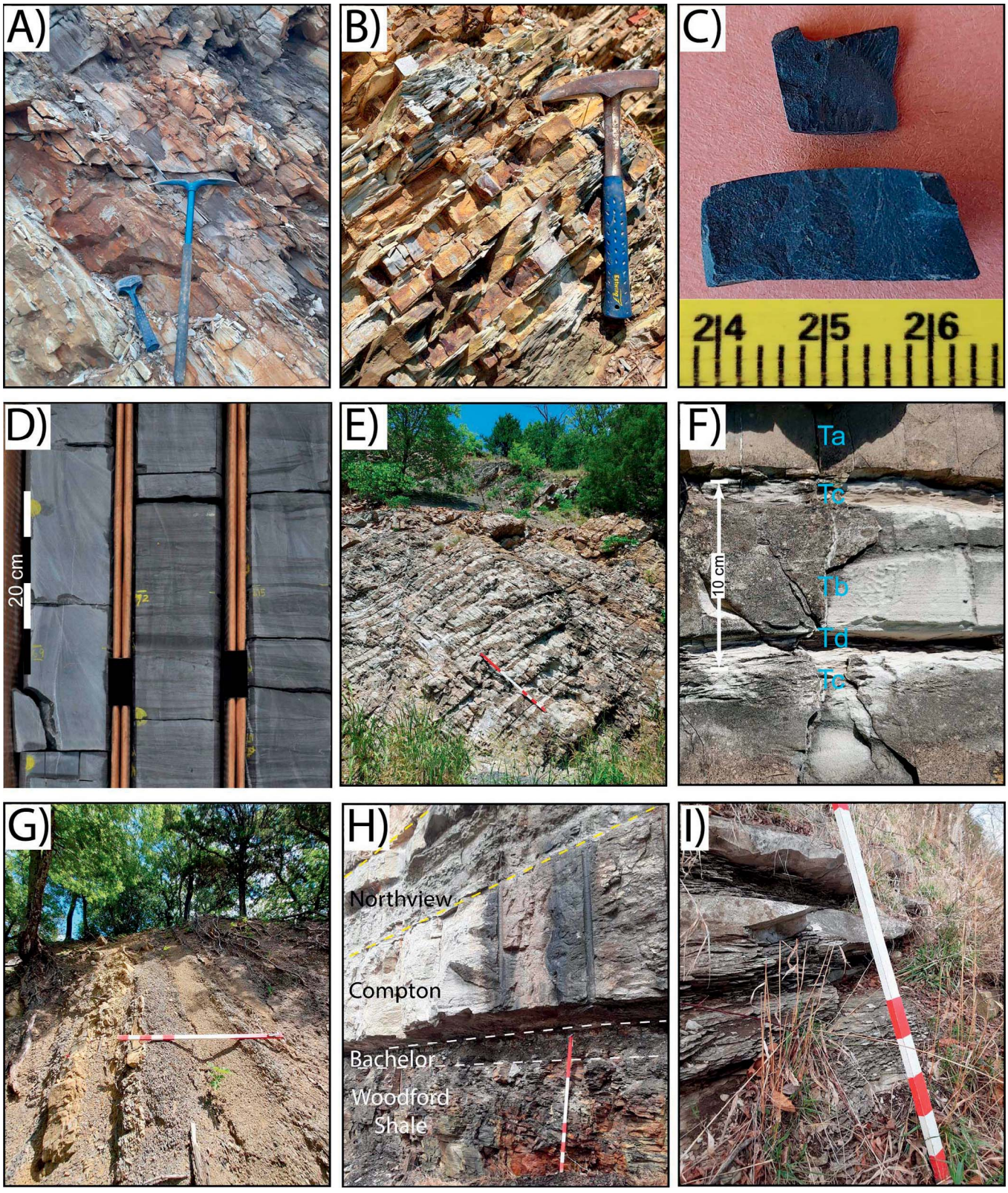

FIG. 5.—Representative outcrop and hand-sample photos across several of the site locations listed in Figure 4. Photos display common features in outcrop and hand sample beforechemical treatments to extract the siliciclastic fraction. **A)** Characteristic laminated mustone beds of the Woodford Shale in southern Oklahoma (No. 9, Fig. 4). **B)** Typical alternating thin beds of chert and laminated to papery shales of the Woodford Shale in the Arbuckle Mountains (No. 8, Fig. 4). **C)** Unweathered black shale core plug fragment of the Woodford Shale extracted from the Barnes Unit D2 core in Major County, Oklahoma (No. 2, Fig. 4). Scale in centimeters. **D)** Massive siltstone and laminated argillaceous siltstone in the Meramec Shaffer core. Core boxes 7–9, depths 2946.70–2949.48 m. Facies interpretation after Miller et al. (2019a) (No. 4, Fig. 4). **E)** First bench of typical repetitive graded siltstone gravity flows of the Sycamore Limestone in southern Oklahoma (No. 8, Fig. 4). **F)** Graded siltstone beds in the Sycamore Limestone at site No. 8 displaying partial Bouma sequences (interpreted Ta, Tb, Tc, Td). **G)** Representative facies in the Caney Shale showing resistive black shale layers with soft brown mudstones and blocky indurated calcareous units (No. 7, Fig. 4). **H)** Representative photo of upper Devonian through Kinderhookian strata in northeastern Oklahoma (No. 15, Fig. 4). **I)** Outcrop of the Bayou Manard Member of the Pryor Creek Formation (No. 15, Fig. 4) displaying calcareous mudstone–wackestone (thick light gray unit) and calcareous platy shales (lithology after Godwin 2017; Godwin and Puckette 2019).

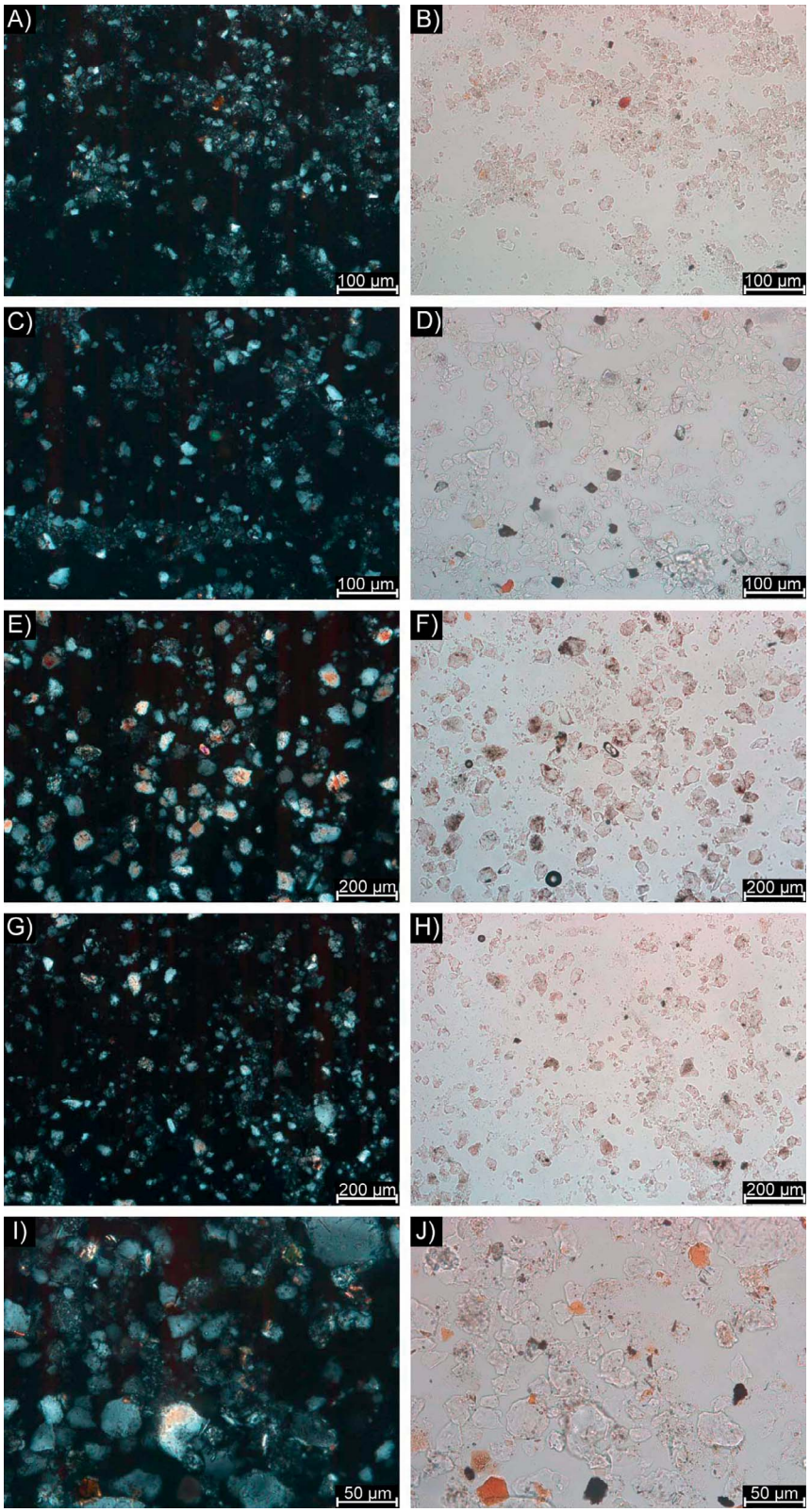

FIG. 6.—Photomicrographs of representative smear slides (in crossed-polarized light (left) and plane-polarized light (right)) of disaggregated siliciclastic fraction from Devono-Mississippian strata in Oklahoma. **A**, **B)** Woodford Shale from the Chenoweth core in northwestern Oklahoma (No. 11, Fig. 4). **C**, **D)** Northview Formation of the St. Joe Group from the Kansas, Oklahoma outcrop (No. 15, Fig. 4). **E**, **F)** Meramec from the Rohling core located just west of central Oklahoma (No. 3, Fig. 4). **G**, **H)** Sycamore Limestone from the Arbuckle Mountains (No. 8, Fig. 4). **I**, **J)** Caney Shale acquired from the Arbuckle Wilderness outcrop (No. 7, Fig. 4). Please see Supplemental File 2 or 4 for location coordinates.

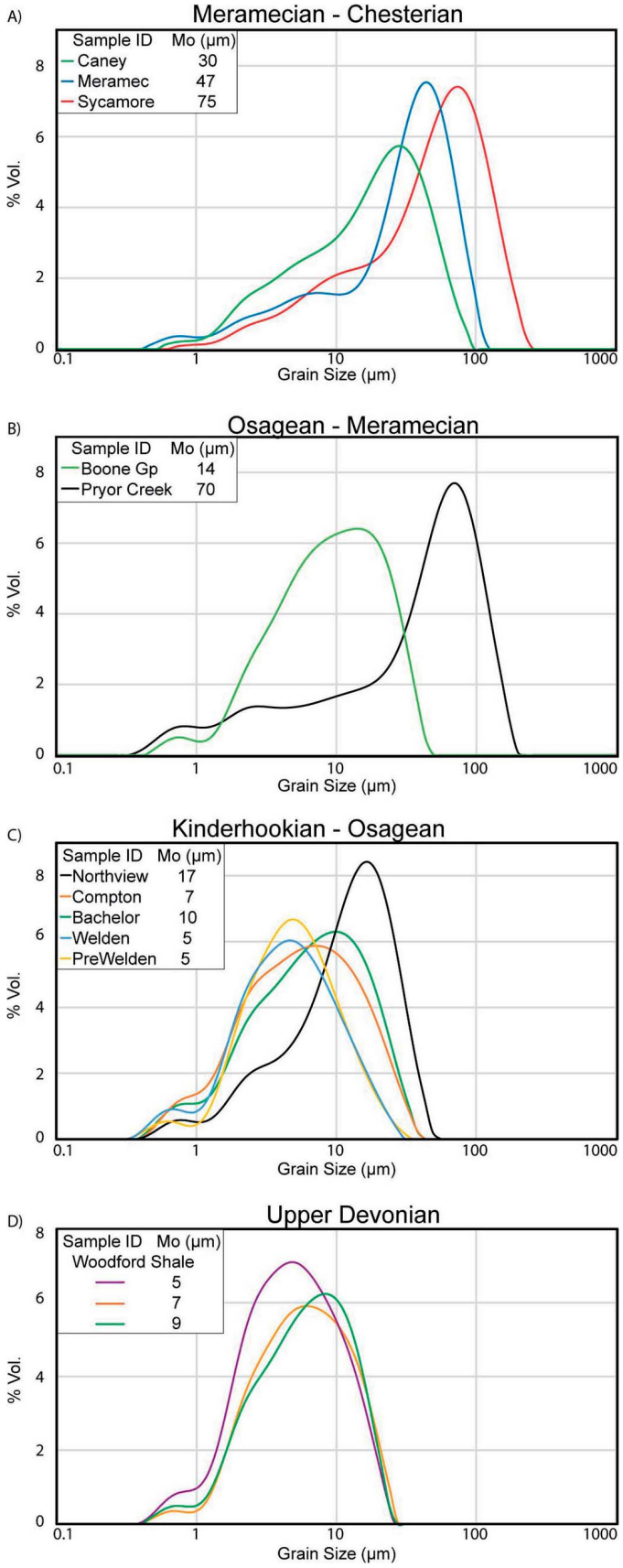

FIG. 7.—Representative particle-size distributions for each of the studied units.

Mississippian. Model performance, the simulated climate evolution throughout the Phanerozoic and comparison to proxy data are presented in Valdes et al. (2021).

ANALYSIS OF THE SILICICLASTIC FRACTION

Analyses of Composition and Grain-Size

Results.—Silicate material from the Woodford Shale contains silt-size quartz, mica, and feldspar (and trace accessory phases), and minor clay. Visual inspection of the coarsest ($> \sim 50$ μm) fraction revealed silicified algal cysts (*Tasmanites*) and, in some cases, mudstone aggregates, both of which were removed before LPSA analysis. Grain-size modes typically range from ~ 5 to 12 μm ($n = 12$). Spatially, the distribution of grain sizes appears generally uniform with a slight coarsening toward north-northwest Oklahoma.

Silicate material from the Mississippian units (Meramec, Sycamore Limestone, Caney Shale, Bachelor Formation, St. Joe Group, and Boone Group) includes quartz, feldspar, biotite, and metamorphic lithic fragments, as well as trace accessory phases (Fig. 6). In general, the older (Kinderhookian–Osagean) units (i.e., Welden Limestone, Bachelor Formation, Northview Formation, Compton Formation) are finer grained (modes of 5–17 μm; two samples from Skaggs core, 34–71 μm) relative to the younger (Meramecian–Chesterian) units (7–83 μm) (Fig. 7; Supplemental File 2).

Interpretation.—The presence of quartz, feldspar, mica, lithic fragments, and accessory silicates (e.g., zircon) confirm the substantial detrital contributions to the study strata (Fig. 6). The Upper Devonian and Lower Mississippian units exhibit the finest modes, whereas Meramecian—Chesterian units are coarser (Fig. 7). The Meramec and Sycamore sections are the siltiest strata by volume of the studied units (Supplemental File 5). All units have modes falling between very fine silt and very fine sand fractions. Such uniformly fine modes are consistent with the hypothesis of eolian transport for this material, addressed further below.

Geochemistry

Results.—Principal-component-analysis (PCA) biplots of major oxides and trace elements (Fig. 8) indicate the relative compositional variability within the dataset depicted by the vectors (Greenacre 2010). The Woodford Shale and Sycamore Limestone occupy distinctly different fields (Fig. 8A), with the Sycamore Limestone displaying significantly greater compositional variability than the silica-rich Woodford Shale. Relative to the North American Shale Composite (NASC) and contemporaneous Appalachian Shale (e.g., Sunbury Shale; Rimmer 2004), samples from both the Woodford Shale and the Sycamore Limestone exhibit depletion in Al_2O_3 but enrichment in SiO_2 (Fig. 8B). From the data illustrated in Figure 8, the siliciclastic fraction of the Sycamore Limestone is compositionally more similar to loess (both modern loess and ancient loessite) than to the NASC (Fig. 8B), especially in siltier layers that compose the upper part of the formation (avg. 85% SiO_2; 6% Al_2O_3; Chemical Index of Alteration of 57–62). Elemental ratios of generally insoluble elements (Zr and Ti, Al oxides) are plotted vs. depth (Fig. 8C) for the Devonian–Mississippian Arbuckle location (Fig. 2, 4). For all three elemental ratios (Zr/TiO_2, Zr/Al_2O_3, and TiO_2/Al_2O_3), values increase abruptly in the lower Sycamore, then return to values comparable to the Woodford but gradually increase again through the middle–upper Sycamore (Fig. 8C).

Interpretation.—The geochemical data confirm the mineralogical evidence for detrital contributions to both the Sycamore Limestone and Woodford Shale. Intriguingly, neither unit overlaps with the North American Shale Composite or the Appalachian Shale, both of which

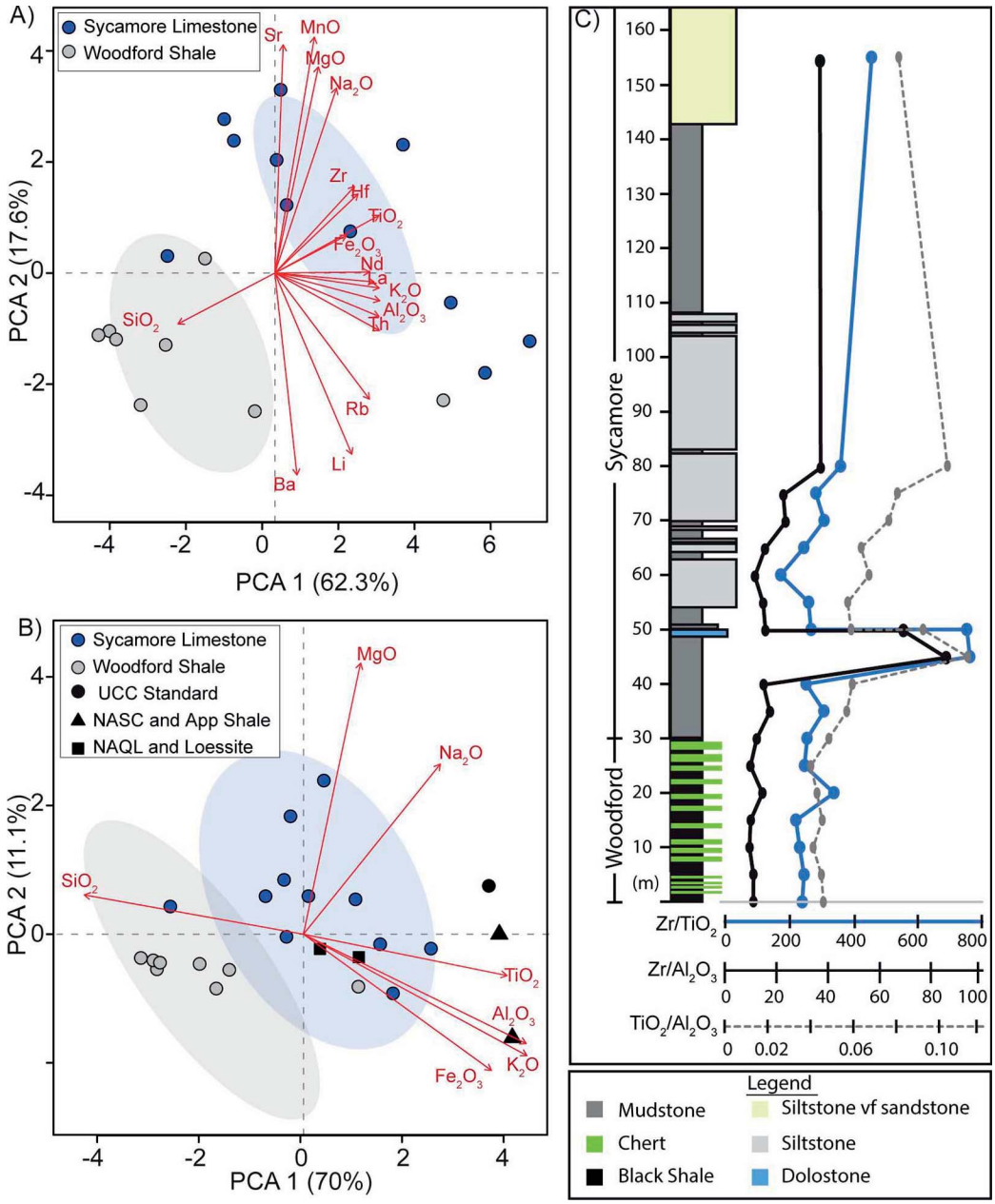

FIG. 8.—PCA biplots and vertical profile of insoluble elements spanning the Woodford Shale and Sycamore Limestone in the southern Arbuckle Mountains (No. 8, Fig. 4). **A)** All major-element and trace-element oxide data showing relative compositional variability between the Woodford Shale (gray) and the Sycamore Limestone (blue). **B)** includes standards comparisons as follows: Upper Continental Crust (UCC) (Taylor and McLennan 1985), North American Shale Composite (NASC) (Gromet et al. 1984), Correlative Sunbury Shale for central Appalachian Basin (Rimmer 2004), North American Quaternary Loess (NAQL) (Taylor et al. 1983), and ancient loessite (Soreghan and Soreghan 2007). **C)** Vertical profile of immobile elements in the Woodford Shale and the Sycamore Limestone outcrop in the southern Arbuckle Mountains. Measured section and lithology of Sycamore Limestone are adapted and modified from Milad et al. (2020).

exhibit much higher values of Al more typical of source material that is highly chemically weathered. Rather, both units—especially the Sycamore Limestone—exhibit a signature more similar to loess (Fig. 8B). The inflection in Zr and TiO_2 with respect to Al_2O_3 ($Zr/Ti\ O_2$, Zr/Al_2O_3, TiO_2/Al_2O_3) in the basal Sycamore Limestone (Fig. 8C) is interpreted to reflect a possible excursion in provenance. These compositional data are independent of grain size, as evinced by the weak relationship ($r^2 < 0.07$) between grain size and these elements (Supplemental File 4), as well as the negligible grain-size variation within each of the Sycamore and Woodford formations in general (Fig. 7).

Detrital-Zircon Geochronology

Results.—U-Pb detrital-zircon ages from the Sycamore Limestone (N = 1; n = 218) and Caney Shale (N = 1; n = 215) yielded a total of 433 concordant to slightly discordant Paleozoic to Archean (age) grains (Fig. 9). Detrital zircon grains recovered for analysis from the Sycamore Limestone are well sorted and considerably finer than 100 μm, while zircons recovered from the Caney Shale are moderately sorted with a majority of the grains finer than 100 μm. Overall, the age spectra for both the Sycamore and Caney units reveal similar age distributions, with detrital

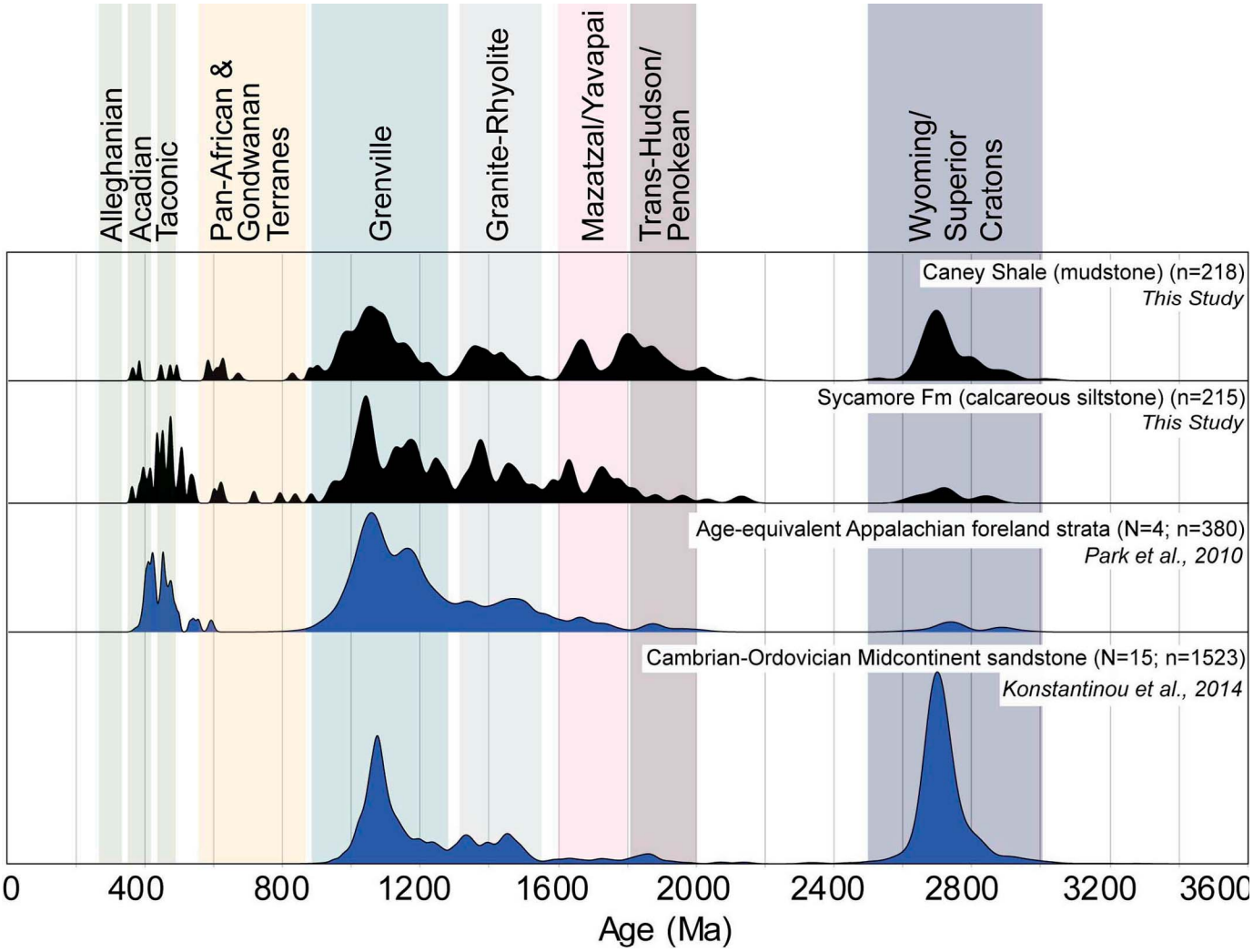

FIG. 9.—Relative age-probability plots of detrital-zircon geochronology results from the Mississippian Sycamore Limestone and Caney Shale from the Arbuckle Mountains in Oklahoma. Also shown for comparison is an average signature for age-equivalent strata from the Appalachian foreland (Park et al. 2010) and an average signature for Cambrian–Ordovician midcontinent sandstone (Konstantinou et al. 2014). Age distributions are divided into potential source-area provinces. The Mississippian Sycamore and Caney Formations from Oklahoma are interpreted to have detrital contributions primarily from Appalachian source areas, including recycled strata and exhumed Appalachian basement (Grenville Province), as well as potential contributions from exhumed Paleoproterozoic and Archean basement.

zircon ages ranging from 365 ± 5 Ma to 3022 ± 12 Ma. The Sycamore Limestone has a primary population of Mesoproterozoic ages (56%), with a primary peak at 1047 Ma and subordinate peaks at 1184, 1382, and 1463 Ma. Secondary populations in the Sycamore unit include Paleoproterozoic ages (16%) with peaks at 1640 Ma and 1739 Ma, as well as early–mid Paleozoic ages (14%) with primary peaks at 449 Ma and 473 Ma, and subordinate peaks at 363, 395, and 507 Ma. The Caney Shale also has a primary detrital-zircon population of Mesoproterozoic ages (38%) with primary peaks at 1062 Ma and 1356 Ma, and secondary populations of Paleoproterozoic ages (26%) with a primary peak at 1817 Ma subordinate peak at 1678 Ma, and Archean ages (23%) with a primary peak at 2715 Ma (Fig. 9).

Interpretation.—Potential source terranes for the siliciclastic fractions of these units include the Archean Superior and Wyoming provinces (> 2.5 Ga) in northern Laurentia, the Trans-Hudson and Penokean provinces (1.8–1.9 Ga) in north-central Laurentia, the Mazatzal–Yavapai (1.6–1.8 Ga), Granite–Rhyolite (1.3–1.5 Ga), and Grenville provinces (0.9–1.3 Ga) throughout central Laurentia and Peri-Gondwanan basement rocks, Pan-African Gondwanan terranes, Taconic plutons, Acadian plutons, and associated synorogenic strata (365–820 Ma) along the Appalachian suture zone in eastern Laurentia (e.g., Hoffman 1989; Van Schmus et al. 1993; Becker et al. 2005; Whitmeyer and Karlstrom 2007; Thomas et al. 2004). The Sycamore Limestone is interpreted to have primary detrital-zircon contributions from the Grenville Province (41%), with secondary contributions from the Granite–Rhyolite province (18%) and Acadian and Taconic plutons from the Appalachian orogen (18%), with minor contributions from the Mazatzal–Yavapai province (13%), Archean provinces (7%), and Trans-Hudson–Penokean provinces (3%; Fig. 9). The Caney Shale is also interpreted to contain primary detrital-zircon contributions from the Grenville Province (33%), but it has secondary contributions from Archean age populations (Wyoming and Superior cratons, or recycled early Paleozoic midcontinent sandstones; 23%), and minor contributions from the Granite–Rhyolite province (12%), Mazatzal–Yavapai province (11%), Appalachian terranes (~11%) and Trans-Hudson–Penokean provinces (~ 9%).

Both the Sycamore and Caney units contain abundant Grenville-age grains (33–40% of total age population) with primary peaks at 1047 Ma

(Sycamore) and 1062 Ma (Caney), which fall in the range of Appalachian Grenville sources (Thomas et al. 2017). Age-equivalent Appalachian foreland strata from Park et al. (2010) also yield abundant Grenville-age detrital zircons with a peak age of 1048 Ma (Fig. 10). In addition, both the Sycamore Limestone and the Caney Shale show contributions (~ 11–18%) from the Taconic and Acadian orogens in the northern Appalachian suture zone, represented by detrital-zircon ages ranging ca. 490–440 Ma and 420–350 Ma (e.g., Thomas et al. 2004, Ettensohn et al. 2019). The Caney Shale did yield significant Archean-age grains, potentially sourced from recycled lower Paleozoic sandstone units from the northern midcontinent and northern Laurentia (Konstantinou et al. 2014).

Simulated Surface Winds

Results.—The paleoenvironmental conditions of the Oklahoma and greater North American mid-continent region changed from predominantly subtropical and arid conditions during the Famennian to a rather monsoonal system exhibiting seasonal wind reversals and summer precipitation during the Early to Middle Mississippian (Kinderhookian through Meramecian). These seasonal wind reversals suggest that the greater midcontinent region was influenced by trade winds during Southern Hemisphere winter months (June through August) (Fig. 10). The simulated surface wind patterns are dominated by an interplay between the prevailing southeasterly trade winds, the land–sea thermal gradient, and local orography. As such, Acadian and Caledonian orogens tend to, in general, guide the flow of air around the landmasses, and absolute wind speeds are reduced due to the presence of these orogenic belts.

Summer winds in the Late Devonian (Fig. 10A) are shown to have come from the south and diverge across the Laurentian epeiric seas with a westerly jet flowing along the northern front of the Acadian orogen. During Late Devonian winter months, a more southeasterly trade-wind circulation developed across Laurentia (Fig. 10B). Westerlies along the southern front of the Acadian orogen show reduced wind values topping over the mountain range with acceleration on the lee side of the orogen. The Osagean (Fig. 10C, D) and Meramecian (Fig. 10E, F) surface-wind patterns are very similar. With the progressive northward movement of Laurentia, the mid-continent region came under the influence of cross-equatorial, northwesterly winds bringing moist air and summer precipitation toward emergent landmasses (Fig. 10E, F). Winter precipitation was very low over the adjacent subtropical land masses and limited to tropical regions northwards of 10° S throughout the Devonian to Mississippian (Supplemental File 6). Surface windflow patterns during the Osagean and Meramecian winter months (JJA) flowed westward along the southern front of the orogen, topped over the range, and swept across the Laurentian epeiric seas in a west to northwestern direction (Fig. 10E, F; Supplemental File 6).

Interpretation.—Model simulations reveal that the Laurentian landmass and associated orogens strongly influenced surface wind patterns. In fact, the presence of a larger landmass at subtropical latitudes during the Early Mississippian promoted seasonal wind reversals and a southward migration of the Intertropical Convergence Zone (ITCZ). According to the model data, a northwestward transport of continental dust toward the midcontinent seems physically plausible, although such a transport would have been possible only during the austral winter months. These months are characterized by northwestward, offshore winds across the potential source regions of the Acadian–Neoacadian clastic wedges.

These wind patterns may be analogous to present winds along the Andean orogen, where westerlies from the South Pacific anticyclone are deflected northward creating a southerly jet along the Andean Pacific front. Air masses top over the orogen and descend as warm dry air off the lee side of the mountain range, known as Zonda winds (Puliafito et al. 2015; Zou and Xi 2021) which are similar in process to Foehn winds off New Zealand's Alps, Chinook winds off the North American Rocky Mountains, and Santa Ana winds over the mountains of southern California (McGowan et al. 1996; Hugenholtz et al. 2007; Álvarez et al. 2021).

Even though coastal and continental summer precipitation increased towards the Early Mississippian, winter months around the orogenic highlands were still dry in the simulations and a stronger easterly wind component may have transported material to the Oklahoma region of Laurentia. A comparable analog for the Early–Middle Mississippian model results, which sits at the same latitude, might be present-day northwestern Australia, where easterlies transport dust westward towards the Indian Ocean during the winter months following the northward migration of the ITCZ (Christensen et al. 2017; Keep et al. 2018).

DISCUSSION

The Enigma of the Missing Proximal Deltas

Delivery of siliciclastic material to epeiric seas occurs by either deltaic or eolian transport. Various processes can then redistribute this material, e.g., hyperpycnal flows, sediment gravity flows induced by slope failure or wave and/or current agitation, or contour currents (Stow et al. 2001; Walsh and Nittrouer 2009; Macquaker et al. 2010; Schieber 2016). Assuming an average wave base of 50 m, Schieber (2016) posited a maximum transport distance of 100 km for remobilized sediment, or up to 400 km for an extreme case of a 200 m wave base. Acknowledging the vast distribution of siliciclastic mud across the Devonian Laurentian sea, Schieber (2016) advocated transport induced by bottom currents, but these arguments demand lateral transport for thousands of kilometers in low-gradient epeiric seas with wave bases << 200 m. While we acknowledge these arguments as one hypothesis, we propose that eolian delivery is an additional and simpler explanation that avoids the need to call upon unknown and unusually powerful storms or tides, as well as flocculation, which is inconsistent with the minimal clay-mineral content of the study units.

The genesis and initial mobilization of the large volumes of ubiquitously fine siliciclastic material characterizing the study units remain unresolved, in large part owing to the absence of proximal feeder system(s). For the Devono-Mississippian Bakken Formation of the Williston Basin, for example, Egenhoff and Fishman (2013) inferred the presence of a deltaic fan that is either not preserved or not exposed. Similar inferences of deltaic feeder systems are applied to Devono-Mississippian mudstone units of the midcontinent (Price et al. 2020) yet without documentation of any remnants of the subaerial (delta plain) or proximal (subaqueous delta) depositional systems. It is highly unlikely that researchers have overlooked such delta systems, given the great density of subsurface data points across the midcontinent region (e.g., > 100,000 wells in Kansas and Oklahoma; Newell et al. 1987; Oklahoma Corporation Commission 2021). The coeval deltas nearest to the midcontinent region during Late Devonian time are the Catskill (Appalachian foreland) and Antler (Antler foreland) systems, and, for the early Mississippian, the Price–Pocono–Grainger–Borden (Appalachians) deltas, that are separated from the midcontinent study area by ~ 1,000–1,500 km (Fig. 3) (Lane and De Keyser 1980; Ausich and Meyer 1990; Gutschick and Sandberg 1991; Richardson and Ausich 2005; Ettensohn 2004, 2008; Ettensohn et al. 2019, 2022).

In contrast to the Upper Devonian, Lower–Middle Mississippian (Kinderhookian–Meramecian) strata in northeastern Oklahoma are cast as a shallow-water carbonate ramp that yielded to the sediment-starved (during Kinderhookian–Osagean) Ouachita trough (southeast) and proto-Anadarko Basin (southwest; Lane and De Keyser 1980; Gutschick and Sandberg 1983; Godwin and Puckette 2019; Miller et al. 2019b). Yet the occurrence of partial Bouma sequences inferred from the Sycamore Limestone (southern Oklahoma) (Schwartzapfel 1990; Miller and Cullen 2018; Milad et al. 2020), as well as clinoform geometries inferred from

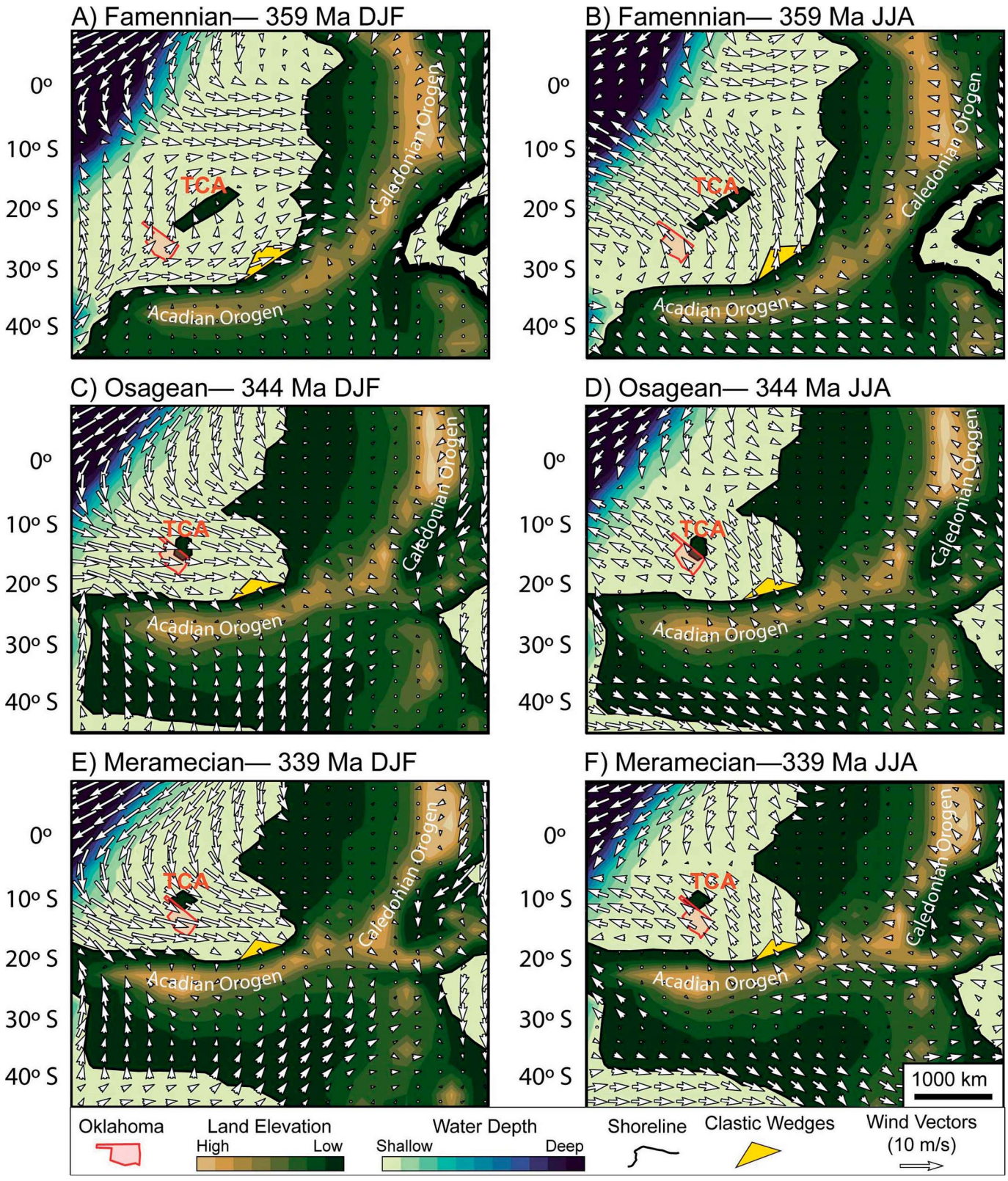

FIG. 10.—Devono-Mississippian wind circulation model simulation time slices. DJF, December–January–February (Austral summer months); JJA, June–July–August (Austral winter months). **A)** Summer months wind vectors during the Late Devonian (Famennian, 359 Ma). **B)** Winter months wind vectors during the Late Devonian (Famennian, 359 Ma). **C)** Summer months wind vectors during the Middle Mississippian (Osagean, 344 Ma). **D)** Winter months wind vectors during the Middle Mississippian (Osagean, 344 Ma). **E)** Summer months wind vectors during the Middle Mississippian (Meramecian, 339 Ma). **F)** Winter months wind vectors during the Middle Mississippian (Meramecian, 339 Ma). Time slice 359 Ma correspond with the Late Devonian Glaciation and the timing of black shale, silt, and chert deposition throughout the North American epeiric sea (Fig. 2). Time slice 344 Ma corresponds with the occurrence of chert in many parts of Laurentia. Time slice 339 Ma corresponds with the general timing of the deposition of the Sycamore Limestone, Meramec, and Caney Shale formations as presented within. TCA, Transcontinental Arch.

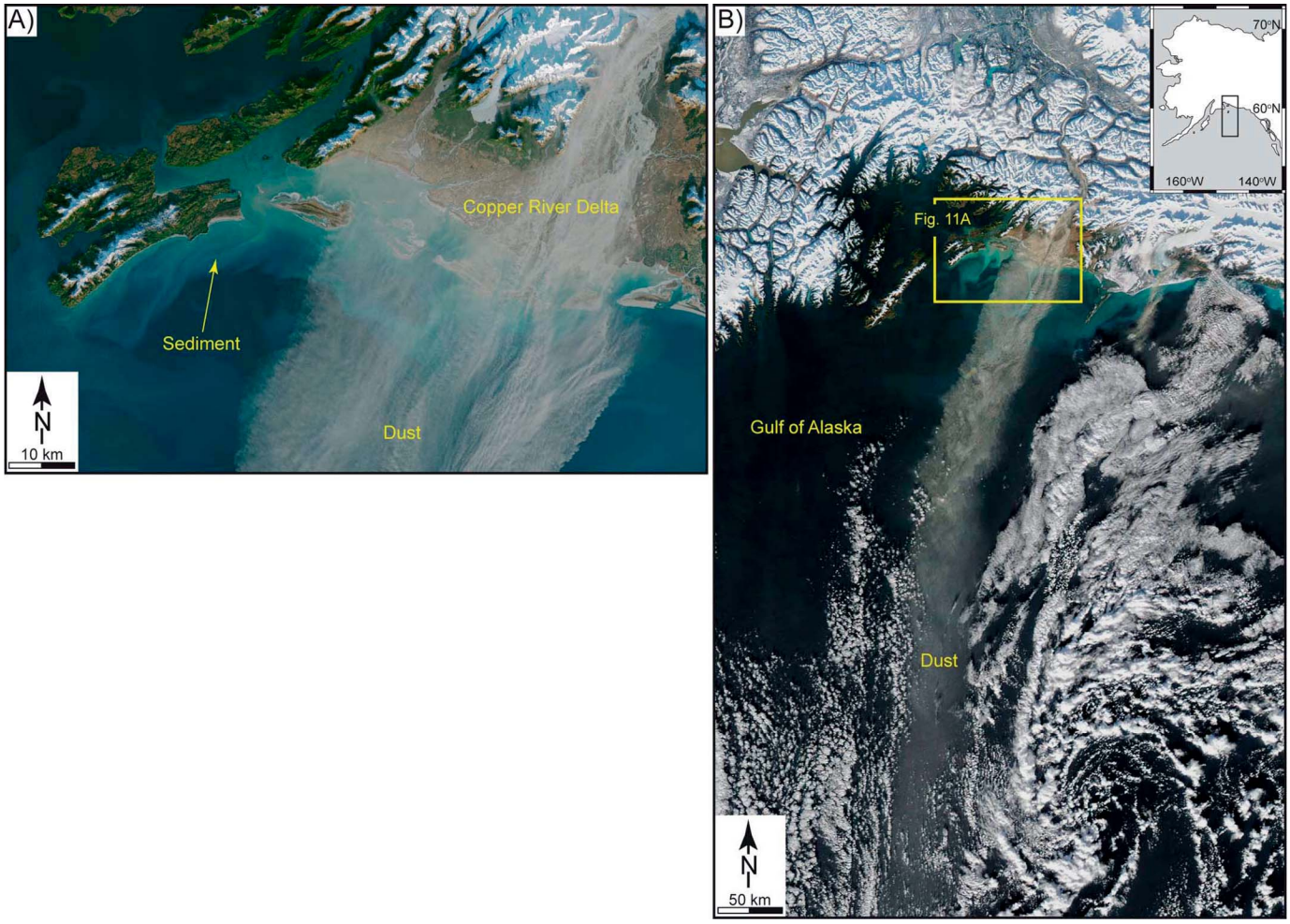

FIG. 11.—Satellite image of sediment plumes emanating off the Copper River Delta (November 2017). **A)** Contrasts the subaqueous sediment plumes versus the eolian plume. **B)** Shows the vast difference in distance eolian plumes travel versus river mouth sediment plumes. Eolian sediment plumes travel up to 10^3 km from source regions, greatly exceeding subaqueous plumes in general. Source of images: NASA Earth Observatory (Stevens 2017a, 2017b).

subsurface data, led Price et al. (2020) to similarly infer a nearby fluvio-deltaic source despite the ubiquitous absence of evidence for proximal feeder systems. The Transcontinental Arch and the Ozark Dome were the most proximal exposed regions during this time but consist of correlative carbonates with limited exposures of Cambro-Ordovician sandstones and localized occurrences of upper Devonian sandstone—insufficient in volume, grain size, and provenance to supply the enormous amounts of exclusively fine-grained material to surrounding regions (Hills and Kottlowski 1983; Bergstrom and Morey 1985; Adler 1986).

If any of these Devono-Mississippian systems were deltaic, they are uniformly "headless"—missing all but the distal-most "prodelta" fines, even where the shelf margins are preserved. In other words, there were no deltaic systems located nearby to transport the siliciclastic material basinward. And if the siliciclastic units represent prodelta fines, they exhibit remarkably uniform grain sizes that fail to fine with distance from the inferred deltaic feeders, and exhibit an unusual dearth of true clay (minerals or grain sizes; Figs. 7, 8).

Origin of Voluminous Mid-Paleozoic Silt

In contrast to the prevalence of fluvio-deltaic inferences for the study units, few have mentioned eolian processes (e.g., Miller and Cullen 2018; Shelley et al. 2019), whilst others make a connection to the origin of chert in correlative units such as the Arkansas Novaculite, the Caballos Novaculite, and cherts of the Osage–Meramecian strata (Banks 1970; Lowe 1976; Cecil 2004, 2018b). Schieber (2016) explicitly dismissed an eolian origin for these mudrocks based on the presumed need for large erg systems to supply the fines via saltation abrasion of sand; yet eolian abrasion produces very little silt (Swet et al. 2019, 2020; Adams and Soreghan 2020). Dust-emitting regions today include both low-subtropical latitude arid regions such as dry lakes of the Bodélé Depression that supply diatomaceous-rich dust (West Africa; Washington et al. 2006; Chappell et al. 2008) and the Nile Delta plain, which fuels the dunes and loess of the Sinai and Negev (Muhs et al. 2013), as well as high-latitude proglacial and periglacial regions, such as the Copper River delta, which seasonally emits large volumes (60–160 ktons in 2006; Crusius et al. 2011) of glacially ground rock powder over hundreds of kilometers into the Gulf of Alaska (Fig. 11). In all of these cases, the fines are inherent to, and emanate from, the (subaerially exposed and desiccated) depositional systems, rather than from eolian saltation.

The critical attributes of the Devono-Mississippian mudrocks of Oklahoma and the greater midcontinent include the: 1) fine grain size restricted to very fine silt to very fine sand with little to no clay (mineral or grain size), 2) blanket-like deposition over large regions, including far from paleocoastlines, 3) deposition in both sediment-starved basins as organic-rich and chert-rich mudstone, and in carbonate ramps as dispersed fines, 4)

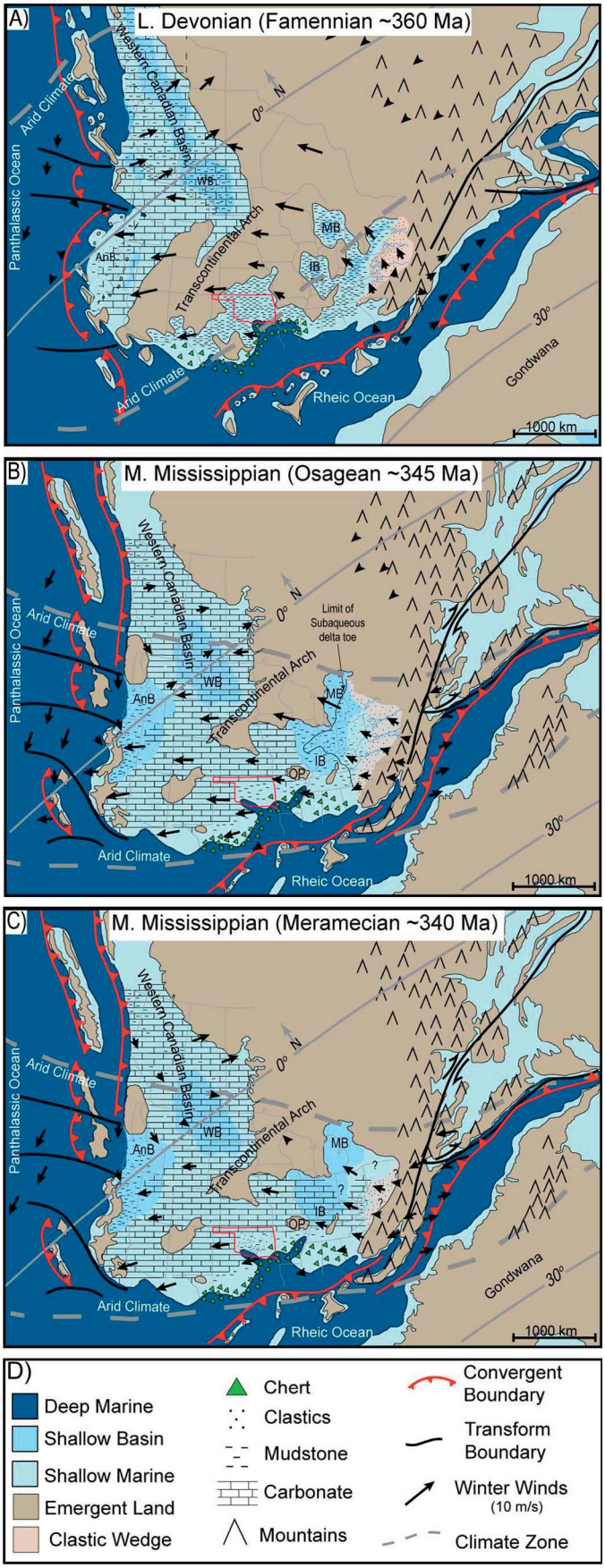

ultimate sources in (primarily) the Appalachian orogen, and 5) enigmatic absence of proximal fluvio-deltaic feeder systems. We propose that delivery of the siliciclastic material to epeiric seas by eolian transport best explains this confluence of attributes.

The predominantly arid and seasonally dry climate in the mostly subtropical latitudes of Devono-Mississippian Laurentia would have favored dust emission. In this model, the Neoacadian Orogen clastic-wedge system (Catskill delta for the Devonian, and Price–Pocono–Borden delta and Mauch Chunk delta for the Mississippian) then provided the source of the material, which was derived from the orogenic highlands. Notably, the Catskill delta system drained (at times) regions thought to have been glaciated during the latest Devonian (Brezinski et al. 2008, 2010; Ettensohn et al. 2020a, 2020b), and thus would have delivered a ready and voluminous source of Al-poor rock flour to the alluvial plain, analogous to the Copper River Delta today (Fig. 11). Although no such glaciation is recorded outside of Gondwanaland for the Mississippian, the subaerial delta plains of the Price–Pocono–Borden–Grainger and Mauch Chunk deltas off the Appalachian Orogen would have supplied abundant silt, analogous to the Nile Delta today. Mass-balance arguments suggest that only 1% (363 km^3) of the total quartz eroded from the Neoacadian orogen and delivered to the Mississippian fluvio-deltaic plains is needed to supply the volume of quartz in the Meramec and Sycamore systems (259 km^3) (Supplemental File 5).

The eolian-delivery model holds that austral winter winds along the Appalachian orogen front and Zonda–Foehn–Chinook-like leeward winds translating into easterlies (Figs. 10, 12) deflated these subaerial delta plains and lofted siliciclastic fines for ultimate deposition into the Laurentian epeiric seas and emergent land regions to the (paleo) north and west (Devonian), and (paleo) west (Mississippian) (Figs. 10, 12). The strength of leeward winds can impose gusty conditions to generate intense dust storms, such as the Zonda winds off the Andes (Norte 2015; Puliafito et al. 2015; Isla et al. 2021), and Chinook winds that rework proglacial strata across the northern Great Plains today (Hugenholtz et al. 2007). This model also explains the dearth of clay minerals (and thus Al), given the lack of intense chemical weathering expected in this arid climate region and—for the latest Devonian—the source in a proglacial delta system.

This model predicts the occurrence of similarly uniform fines distributed in coeval units across a large region of the Laurentian epeiric sea, as indeed occurs (Figs. 2, 3). Additionally, it builds on several other examples of eolian–marine units posited for similarly enigmatic, fine-grained (and generally clay-poor) siliciclastic systems that lack fluvio-deltaic components, such as those of the Permian Delaware Mountain Group (Fischer and Sarnthein 1988), Phosphoria Formation (Carroll et al. 1998), various units of the Permo-Pennsylvanian (Soreghan 1992; Soreghan et al. 2008), and Lower Mississippian units of the Appalachian Basin (Cecil et al. 2018a). Similarly, it builds on the eolian-dust model for the origin of chert in Paleozoic units of Laurentia proposed by Lowe (1976) and Cecil et al. (2018b).

←

FIG. 12.—Summary figure of paleogeographic reconstructions from Figure 3 with posted austral winter (JJA) surface wind vectors from Figure 10. Oklahoma is outlined in red. **A)** Latest Devonian (Famennian, ~ 360 Ma). The Catskill Delta complex is indicated by a stippled beige polygon with sketched fluvial systems. **B)** Middle Mississippian Ma (Osagean, ~ 345). The Price–Pocono Delta complex is also noted by a stippled beige polygon with sketched fluvial systems. **C)** Middle Mississippian (Meramecian, ~ 340 Ma). **D)** Legend. Each panel shows the midcontinent region in the subtropical arid climate belt, in the orographic rain shadow of the Appalachian orogen, and far removed from shorelines. Paleowind directions emanate from the southeast across the Appalachian clastic wedges. Paleogeographic maps were constructed from Blakey (2013), North American Key Time Slices ©2013 Colorado Plateau Geosystems, Inc. as base maps, with paleoclimate data from sources including Boucot et al. (2013) and Scotese and Wright (2018). See Supplemental File 2 for map construction references.

The Woodford Shale consistently exhibits the finest modes of the study units and the highest silica content (Figs. 7, 8). Its uniquely high silica content is commonly attributed to the influence of biogenic silica from nutrient-rich upwelling (Turner et al. 2016), but this explanation evades the root issue of an ultimate Si source. Cecil et al. (2018b) posited that much Phanerozoic chert was likely sourced by eolian dust; this model seems viable for the Woodford Shale given the paleogeographic context of arid conditions across the midcontinent of Laurentia during the Late Devonian, conducive to the availability and transport of ultrafine siliceous dust. We propose that the fine detrital modes reflect: 1) the distance to source and 2) the direction of surface wind circulation patterns, given the significant paleogeographic shifts from Late Devonian to Early–Middle Mississippian times (Figs. 10, 12). During the Late Devonian, Oklahoma and the greater midcontinent seaway were situated west-northwest of the Catskill delta at $\sim 30^{\circ}$ S. Prevailing winds off the leeward front of the Appalachian orogen would have transported eolian dust in a north and west-northwesterly direction, across the North American midcontinent to Oklahoma and beyond. The emergent transcontinental arch may have provided temporary storage areas along this path.

Ultimately, the finest fraction accumulated in the Woodford Shale; by the Mississippian, shifts occurred in both the location of the primary source (now the Price–Pocono–Borden–Grainger, the Mauch Chunk deltas, and coastal clastic systems) and the paleolatitude ($\sim 15^{\circ}$ northward). By this time, the Price–Pocono–Borden–Grainger and Mauch Chunk deltas were east-southeast of Oklahoma, enabling prevailing easterlies to loft fines from these systems directly into the epeiric seas across the greater midcontinent. With the northward drift of the Laurentian continent, Southern Hemisphere winter winds off the Appalachian orogen shifted to blow more directly toward the west and west-northwest (less circuitous than those of the Late Devonian). This shift might explain the elevated grain sizes, higher volume of quartz, and more "loess-like" signature in the Meramecian samples of the Meramec and Sycamore (Fig. 8). Additionally, orographic effects of the greater Appalachian orogen presumably further exacerbated the aridity across Laurentia, leading to enhanced eolian emissions.

Finally, widespread delivery of only minimally (chemically) weathered eolian fines to Devono-Mississippian epeiric seas may have had auxiliary effects on organic carbon in these systems. The Mississippian (and Upper Devonian) of North America contain anomalously high organic carbon, with the Woodford Shale and correlatives considered world-class source rocks (Ulmishek and Klemme 1990; Kuuskraa 2011; Sonnenberg 2011). We speculate that this remarkable organic richness might reflect eolian delivery of abundant nutrients (notably iron) to these distal epeiric seas, stimulating productivity and associated preservation of organic carbon, as has been observed in the Bering Sea (Koffman et al. 2021) and suggested in other deep-time, dust-sourced systems (e.g., Carroll et al. 1998; Gabbott et al. 2010; Sur et al. 2015; Abadi et al. 2020).

CONCLUSIONS

- Siliciclastic silt and mudstone are common throughout Upper Devonian–Lower Mississippian epeiric-sea strata of Laurentia, but no proximal fluvial–deltaic feeder systems exist to explain transport of this material.
- Mineralogical data indicate a clear detrital source. Grain-size modes range from very fine silt to very fine sand, with minimal lateral variation in units across broad swaths of Oklahoma and the greater midcontinent region. Geochemical signatures are Si-rich and Al-poor, reflective a dearth of clay minerals (particularly Woodford Shale and Sycamore systems). Detrital-zircon geochronology indicates primary sources in the Appalachian orogen.
- Paleogeographic reconstructions show that the midcontinent occupied the subtropical arid belt, in the orographic rain shadow of the growing Appalachian orogen. Consequent aridity would have promoted dust emission from vast delta plains draining the Appalachian highlands. Model simulations of surface wind circulations indicate that Southern Hemisphere winter months were conducive for eolian delivery of fine siliciclastic material toward the west and northwest, derived from Appalachian clastic wedges. Alpine glaciation in these highlands during at least the latest Devonian produced large volumes of physically weathered fines.
- Siliciclastic silt of the Upper Devonian Woodford Shale most likely experienced a circuitous eolian trajectory and greater transport distances, resulting in the predominance of very fine silt modes. In contrast, Mississippian units were directly downwind of deltaic plains of the northern Appalachian system, resulting in generally coarser silt to very fine sand modes.
- Coeval units located most distally contain abundant chert, consistent with sourcing from very fine silica dust. Eolian transport of material that was minimally chemically weathered to Devono-Mississippian epeiric seas likely delivered essential nutrients that stimulated organic productivity in these commonly organic-rich units—a hypothesis that merits further investigation.

SUPPLEMENTAL MATERIAL

Supplemental material is available from the SEPM Data Archive: https://www.sepm.org/supplemental-materials.

ACKNOWLEDGMENTS

This paper grew out of a graduate student seminar in the School of Geosciences at the University of Oklahoma led by Drs. Lynn Soreghan and Andrew Cullen. We thank the University of Oklahoma School of Geosciences, the Eberly Family Chair (Soreghan), and Warwick Energy (Cullen) for funding, Vyetta Jordan and the Oklahoma Petroleum Information Center (OPIC) for access to core, Cody Totten for contributions to initial data collection, the University of Arizona LaserChron Center NSF grant (NSF-EAR 1649254) for detrital-zircon acquisition and Mehrdad Sardar Abadi for discussions. We thank the reviewers and editors for their constructive comments on earlier versions of this manuscript. We also thank Patrick Kelly and Oluwatobiloba Francis Oyebanji for assistance with field data acquisition.

REFERENCES

Abadi, M.S., Owens, J.D., Liu, X., Them, T.R., Cui, X., Heavens, N.G., and Soreghan, G.S., 2020, Atmospheric dust stimulated marine primary productivity during Earth's penultimate icehouse: Geology, v. 48, p. 247–251.

Adams, J.E., 1965, Stratigraphic-tectonic development of Delaware Basin: American Association of Petroleum Geologists, Bulletin, v. 49, p. 2140–2148.

Adams, S.M., and Soreghan, G.S., 2020, A test of the efficacy of sand saltation for silt production: implications for the interpretation of loess: Geology, v. 48, p. 1105–1109.

Adler, F.J., 1986, Mid-continent region, *in* Childs, O.E., Steele, G., Salvador, A., and Lindberg, F.A., eds., Correlation of Stratigraphic Units of North America: American Association of Petroleum Geologists, Correlation of Stratigraphic Units in North America, chart MC.

Álvarez, C.A., Carbajal, N., and Pineda-Martínez, L.F., 2021, Dust pollution caused by an extreme Santa Ana wind event: Natural Hazards, v. 110, p. 1–16.

Andrews, R.D., 2007, Stratigraphy, production, and reservoir characteristics of the Caney Shale in southern Oklahoma: Shale Shaker, v. 58, p. 9–25.

Angulo, S., and Buatois, L.A., 2012, Integrating depositional models, ichnology, and sequence stratigraphy in reservoir characterization: the middle member of the Devonian–Carboniferous Bakken Formation of subsurface southeastern Saskatchewan revisited: American Association of Petroleum Geologists, Bulletin, v. 96, p. 1017–1043.

Ausich, W.I., and Meyer, D.L., 1990, Origin and composition of carbonate buildups and associated facies in the Fort Payne Formation (Lower Mississippian, south-central Kentucky): an integrated sedimentologic and paleoecologic analysis: Geological Society of America, Bulletin, v. 102, p. 129–146.

Ballard, W.W., Bluemie, J.P., and Gerhard, L.C., 1983, Northern Rockies/Williston Basin Region Correlation Chart, *in* Childs, O.E., Steele, G., Salvador, A., and Lindberg, F.A., eds., Correlation of Stratigraphic Units of North America: American Association of Petroleum Geologists, Correlation of Stratigraphic Units in North America, chart NRW.

Banks, N.G., 1970, Nature and origin of early and late cherts in the Leadville Limestone, Colorado: Geological Society of America, Bulletin, v. 81, p. 3033–3048.

Barrows, M.H., and Cluff, R.M., 1984, New Albany Shale Group (Devonian–Mississippian) source rocks and hydrocarbon generation in the Illinois Basin, *in* Demaison, G.D., and Roelef, J., eds., Petroleum Geochemistry and Basin Evaluation: American Association of Petroleum Geologists, Memior 35, p. 111–138.

Becker, T.P., Thomas, W.A., Samson, S.D., and Gehrels, G.E., 2005, Detrital zircon geochronology of the southern Appalachian foreland basin and its source rocks: Sedimentary Geology, v. 182, p. 59–86.

Bergstrom, D.J., and Morey, G.B., 1985, Northern mid-continent region, *in* Childs, O.E., Steele, G., Salvador, A., and Lindberg, F.A., eds., Correlation of Stratigraphic Units of North America: American Association of Petroleum Geologists, Correlation of Stratigraphic Units in North America, chart NMC.

Blakey, R.C., 2013, North America Key Time Slices © 2013: Colorado Plateau Geosystems, Inc.

Boardman, D.R., Thompson, T.L., Godwin, C., Mazzullo, S.J., Wilhite, B.W., and Morris, B.T., 2013, High-resolution conodont zonation for Kinderhookian (Middle Tournasian) and Osagean (Upper Tournasian–Lower Visean) strata of the western edge of the Ozark Plateau, North America: Shale Shaker, v. 64, p. 98–151.

Boswell, R.M., and Donaldson, A.C., 1988, Depositional architecture of the Upper Devonian Catskill delta complex: central Appalachian basin, U.S.A., *in* McMillan, N.J., Embry, A.F., and Glass, D.J., eds., Devonian of the World: Canadian Society of Petroleum Geologists, Memoir 14, v. 2, p. 65–84.

Boucot, A.J., Xu, C., Scotese, C.R., and Morley, R.J., 2013, Phanerozoic Paleoclimate: An Atlas of Lithologic Indicators of Climate: SEPM, Concepts in Sedimentology and Paleontology, no. 11, 478 p.

Branch, J., 1988, Conodonts from the Welden Limestone (Osagean, Mississippian), south central Oklahoma [MS Thesis]: Texas Tech University, Lubbock, 126 p.

Brezinski, D.K., Cecil, C.B., Skema, V.W., and Stamm, R., 2008, Late Devonian glacial deposits from the eastern United States signal an end of the mid-Paleozoic warm period: Palaeogeography, Palaeoclimatology, Palaeoecology, v. 268, p. 143–151.

Brezinski, D.K., Cecil, C.B., Skema, V.W., and Kertis, C.A., 2009, Evidence for long-term climate change in Upper Devonian strata of the central Appalachians: Palaeogeography, Palaeoclimatology, Palaeoecology, v. 284, p. 315–325.

Brezinski, D.K., Cecil, C.B., and Skema, V.W., 2010, Late Devonian glacigenic and associated facies from the central Appalachian Basin, eastern United States: Geological Society of America, Bulletin, v. 122, p. 265–281.

Campbell, J.A., Mankin, C.J., Scwarzkopf, A.B., and Raymer, J.H., 1988, Habitat of petroleum in Permian rocks of the midcontinent region, *in* Morgan, W.A., and Babcock, J.A., eds., Permian Rocks of the Midcontinent: SEPM, Midcontinent Section, Special Publication 1, p. 13–35.

Caputo, M.V., de Melo, J.H.G., Streel, M., and Isbell, J.L., 2008, Late Devonian and Early Carboniferous glacial records of South America, *in* Fielding, C.R., Frank, T.D., and Isbell, J.L., eds., Resolving the Late Paleozoic Ice Age in Time and Space: Geological Society of America, Special Publication 441, p. 161–173.

Carroll, A.R., Stephens, N.P., Hendrix, M.S., and Glenn, C.R., 1998, Eolian-derived siltstone in the Upper Permian Phosphoria Formation: implications for marine upwelling: Geology, v. 26, p. 1023–1026.

Cecil, C.B., 2004, Eolian dust and the origin of sedimentary chert: U.S. Geological Survey, Open-File Report 2004-1098, 15 p

Cecil, C., DiMichele, W.A., Rahl, J.M., Eble, C., and Stamm, R.G., 2018a, The Devonian–Mississippian climate transition in southeastern Laurentia (Eastern USA): late Famennian glaciation, Kinderhookian coal, Osagean loess [Abstract]: Geological Society of America, Abstracts with Programs, v. 50, no. 6.

Cecil, C., Hemingway, B.S., and Dulong, F.T., 2018b, The chemistry of eolian quartz dust and the origin of chert: Journal of Sedimentary Research, v. 88, p. 743–752.

Chappell, A., Warren, A., O'Donoghue, A., Robinson, A., Thomas, A., and Bristow, C., 2008, The implications for dust emission modeling of spatial and vertical variations in horizontal dust flux and particle size in the Bodélé Depression, Northern Chad: Journal of Geophysical Research: Atmospheres, v. 113, no. DO4214.

Christensen, B.A., Renema, W., Henderiks, J., De Vleeschouwer, D., Groeneveld, J., Castañeda, I.S., Reuning, L., Bogus, K., Auer, G., Ishiwa, T., and McHugh, C.M., 2017, Indonesian throughflow drove Australian climate from humid Pliocene to arid Pleistocene: Geophysical Research Letters, v. 44, p. 6914–6925.

Cohen, K.M., Finney, S.C., Gibbard, P.L., and Fan, J.-X., 2013, The ICS International Chronostratigraphic Chart, Updated (v. 2022) Episodes, v. 36, p. 199–204.

Connock, G.T., Nguyen, T.X., and Philp, R.P., 2018, The development and extent of photic-zone euxinia concomitant with Woodford Shale deposition: American Association of Petroleum Geologists, Bulletin, v. 102, p. 959–986.

Craig, L.C., Connor, C.W., and Armstrong, A.K., 1978, Paleotectonic investigations of the Mississippian System in the United States: U.S. Geological Survey, Professional Paper 1010, 559 p.

Crusius, J., Schroth, A.W., Gasso, S., Moy, C.M., Levy, R.C., and Gatica, M., 2011, Glacial flour dust storms in the Gulf of Alaska: hydrologic and meteorological controls and their importance as a source of bioavailable iron: Geophysical Research Letters, v. 38, no. L06602 doi:10.1029/ 2010GL046573.

Dalziel, I.W.D., 1991, Pacific margins of Laurentia and East Antarctica as a conjugate rift pair: evidence and implications for an Eocambrian supercontinent: Geology, v. 19, p. 598–601.

Domeier, M., and Torsvik, T.H., 2014, Plate tectonics in the late Paleozoic: Geoscience Frontiers, v. 5, p. 303–350.

Duarte, D., Milad, B., Elmore, R.D., Pranter, M.J., and Slatt, R., 2021, Diagenetic controls on reservoir quality of a mixed carbonate–siliciclastic system: Sycamore Formation, Sho-Vel-Tum Field, Oklahoma, USA: Marine and Petroleum Geology, v. 134, no.105375.

Egenhoff, S.O., and Fishman, N.S., 2013, Traces in the dark: sedimentary processes and facies gradients in the upper shale member of the Upper Devonian–Lower Mississippian Bakken Formation, Williston Basin, North Dakota, USA: Journal of Sedimentary Research, v. 83, p. 803–824.

Elias, M.K., 1956, Upper Mississippian and Lower Pennsylvanian formations of south-central Oklahoma, *in* Hicks, I.C., Westheimer, J., Tomlinson, C.W., Putnam, D.M., and Selk, E.L., eds., Petroleum Geology of Southern Oklahoma, v. 1: American Association of Petroleum Geologists, Special Publication 16, p. 56–134.

Ettensohn, F.R., 2004, Modeling the nature and development of major Paleozoic clastic wedges in the Appalachian Basin, USA: Journal of Geodynamics, v. 37, p. 657–681.

Ettensohn, F.R., 2008, The Appalachian foreland basin in eastern United States, *in* Miall, A.D., ed., The Sedimentary Basins of the United States and Canada: The Sedimentary Basins of the World: Amsterdam, Elsevier, v. 5, p. 105–179.

Ettensohn, F.R., and Woodrow, D.L., 1985, The Catskill delta complex and the Acadian orogeny: a model, *in* Woodrow, D.L., and Sevon, W.D., eds., The Catskill Delta: Geological Society of America, Special Paper 201, p. 39–49.

Ettensohn, F.R., Pashin, J.C., and Gilliam, W., 2019, The Appalachian and Black Warrior basins: foreland basins in the eastern United States, *in* Miall, A., ed., The Sedimentary Basins of the United States and Canada: Amsterdam, Elsevier, v. 2 p. 129–237.

Ettensohn, F.R., Clayton, G., Lierman, R.T., Mason, C.E., Krause, F.F., Debuhr, C., Brackman, T.B., Anderson, E.D., Dennis, A.J., and Pashin, J.C., 2020a, Late Devonian lonestones, diamictites, and coeval black shales from the Appalachian Basin: discerning relationships and implications for Late Devonian Appalachian history and glacially driven seafloor anoxia, *in* Avary, K.L., Hasson, K.O., and Diecchio, R.J., eds., The Appalachian Geology of John M. Dennison: Rocks, People, and a Few Good Restaurants along the Way: Geological Society of America, Special Paper 545, p. 67–88.

Ettensohn, F.R., Seckinger, D.C., Eble, C.F., Clayton, G., Li, J., Martins, G.A., Hodelka, B.N., Lo, E.L., Harris, F.R., and Taghizadeh, N., 2020b, Age and tectonic significance of diamictites at the Devonian–Mississippian transition in the central Appalachian Basin, *in* Swezey, C.S., and Carter, M.W., eds., Geology Field Trips in and around the U.S. Capital: Geological Society of America, Field Guide 57, p. 79–103.

Ettensohn, F.R., Gilliam, W., Li, J., and Zeng, M., 2022, Timing and evolution of the Mississippian sedimentary system on southeastern Laurussia: evidence from the Appalachian area, USA: Palaeogeography, Palaeoclimatology, Palaeoecology, v. 591, p. 110874.

Feinstein, S., 1981, Subsidence and thermal history of Southern Oklahoma Aulacogen: implications for petroleum exploration: American Association of Petroleum Geologists, Bulletin, v. 65, p. 2521–2533.

Fischer, A.G., and Sarnthein, M., 1988, Airborne silts and dune-derived sands in the Permian of the Delaware Basin: Journal of Sedimentary Petrology, v. 58, p. 637–643.

Foster, G.L., Royer, D.L., and Lunt, D.J., 2017, Future climate forcing potentially without precedent in the last 420 million years: Nature Communications, v. 8, p. 1–8.

Foster, T.M., Soreghan, G.S., Soreghan, M.J., Benison, K.C., and Elmore, R.D., 2014, Climatic and paleogeographic significance of eolian sediment in the Middle Permian Dog Creek Shale (Midcontinent US): Palaeogeography, Palaeoclimatology, Palaeoecology, v. 402, p. 12–29.

Gabbott, S.E., Zalasiewicz, J., Aldridge, R.J., and Theron, J.N., 2010, Eolian input into the Late Ordovician postglacial Soom Shale, South Africa: Geology, v. 38, p. 1103–1106.

Gehrels, G.E., 2010, Excel macros: normalized age probability plots, Cumulative age Probability Plots, KT test: University of Arizona, Arizona LaserChron Center, Tucson, https://docs.google.com/View?id=dcbpr8b2_7c3s6pxft.

Gehrels, G., and Pecha, M., 2014, Detrital zircon U-Pb geochronology and Hf isotope geochemistry of Paleozoic and Triassic passive margin strata of western North America: Geosphere, v. 10, p. 49–65.

Godwin, C.J., 2017, Lithostratigraphy and conodont biostratigraphy of the Upper Boone Group and Mayes Group in the southwestern Ozarks of Oklahoma, Missouri, Kansas, and Arkansas [Ph.D. Thesis]: Oklahoma State University, Stillwater, 321 p.

Godwin, C.J., and Puckette, J.O., 2019, Depositional cyclicity within the Mayes Group (Meramecian–Chesterian) along the western edge of the Mississippian outcrop belt in northeastern Oklahoma, *in* Grammer, G.M., Gregg, J.M., Puckette, J.O., Jaiswal, P., Mazzullo, S.J., Pranter, M.J., and Goldstein, R.H., eds., Mississippian Reservoirs of the Midcontinent: American Association of Petroleum Geologists, Memoir 122, p. 107–130.

Godwin, C.J., Boardman, D.R., II, and Puckette, J.O., 2019, Meramecian–Chesterian (upper Viséan) conodont biostratigraphy and revised lithostratigraphy along the southwestern flank of the Ozark uplift, southern midcontinent, U.S.A., *in* Grammer, G.M., Gregg, J.M., Puckette, J.O., Jaiswal, P., Mazzullo, S.J., Pranter, M.J., and Goldstein, R.H., eds., Mississippian Reservoirs of the Midcontinent: American Association of Petroleum Geologists, Memoir 122, p. 59–88.

Gromet, L.P., Dymek, R.F., Haskin, L.A., and Korotev, R.L., 1984, North American shale composite: its compilation, major and trace element characteristics: Geochimica et Cosmochimica Acta, v. 48, p. 2469–2482, doi:10.1016/0016-7037(84)90298-9.

Greenacre, M., 2010, Biplots in Practice: Fundacîon BBVA, Rubes Editorial.

Gutschick, R.C., and Sandberg, C.A., 1983, Mississippian continental margins of the conterminous United States, *in* Stanley, D.J., and Moore, G.T., eds., The Shelfbreak: Critical Interface on Continental Margins: SEPM, Special Publication 33, p. 79–96.

Gutschick, R.C., and Sandberg, C.A., 1991, Late Devonian history of Michigan Basin, *in* Catacosinos, P.A., and Daniels, P.A., Jr., eds., Early Sedimentary Evolution of the Michigan Basin: Geological Society of America, Special Paper 256, p. 203–220.

Higley, D.K., 2013, 4D Petroleum system model of the Mississippian System in the Anadarko Basin Province, Oklahoma, Kansas, Texas, and Colorado, USA: The Mountain Geologist, v. 50, p. 81–98.

Hills, J.H., and Kottlowski, F.E., 1983, Southwest/southwest mid-continent region *in* Childs, O.E., Steele, G., Salvador, A., and Lindberg, F.A., eds., Correlation of Stratigraphic Units of North America: American Association of Petroleum Geologists, Correlation of Stratigraphic Units in North America, chart SSMC.

Hintze, L.F., 1985, Great Basin region, *in* Childs, O.E., Steele, G., Salvador, A., and Lindberg, F.A., eds., Correlation of Stratigraphic Units of North America: American Association of Petroleum Geologists, Correlation of Stratigraphic Units in North America, chart GB.

Hoffman, P.F., 1989, Precambrian geology and tectonic history of North America, *in* Bally, A.W., and Palmer, A.R., eds., The Geology of North America: An Overview: Geological Society of America, p. 447–512.

Hugenholtz, C.H., Wolfe, S.A., and Moorman, B.J., 2007, Sand–water flows on cold-climate eolian dunes: environmental analogs for the eolian rock record and Martian sand dunes: Journal of Sedimentary Research, v. 77, p. 607–614.

Isaacson, P.E., Díaz-Martínez, E., Grader, G.W., Kalvoda, J., Bábek, O., and Devuyst, F.X., 2008, Late Devonian–earliest Mississippian glaciation in Gondwanaland and its biogeographic consequences: Palaeogeography, Palaeoclimatology, Palaeoecology, v. 268, p. 126–142.

Isla, F.I., Isla, M., Bertola, G., and Bedmar, J.M., 2021, Taton dune field: wind selection across the Southamerican arid diagonal, Puna Argentina: Quaternary and Environmental Geosciences, v. 12, p. 19–29.

Jiang, Z., and Liu., 2011, A pretreatment method for grain size analysis of red mudstones: Sedimentary Geology, v. 241, p. 13–21.

Johnson, J.G., and Pendergast, A., 1981, Timing and mode of emplacement of the Roberts Mountains allochthon, Antler orogeny: Geological Society of America, Bulletin, v. 92, p. 648–658.

Johnson, K.S., Amsden, T.W., Denison, R.E., Dutton, S.P., Goldstein, A.G., Rascoe, B., Jr., Sutherland, P.K., and Thompson, D.M., 1988, Southern midcontinent region, *in* Sloss, L.L., ed., Sedimentary Cover, North American Craton, U.S: Geological Society of America, p. 307–359.

Johnson, K.S., Amsden, T.W., Dennison, R.E., Dutton, S.P., Goldstein, A.G., Roscoe, B., Sutherland, P.K., and Thompson, D.M., 1989, Geology of the southern midcontinent: Oklahoma Geological Survey, Special Publication 89-2, p. 1–53.

Keep, M., Holbourn, A., Kunht, W., and Gallagher, S.J., 2018, Progressive Western Australian collision with Asia: implications for regional orography, oceanography, climate and marine biota: Royal Society of Western Australia, Journal, v. 101, p. 1–17.

Kent, H.C., Couch, E.L., and Kneep, R.A., 1988, Central and southern Rockies region, *in* Childs, O.E., Steele, G., Salvador, A., and Lindberg, F.A., eds., Correlation of Stratigraphic Units of North America: American Association of Petroleum Geologists, Correlation of Stratigraphic Units in North America, chart CSR.

Kirkland, D.W., Denison, R.E., Summer, D.M., and Gormly, J.R., 1992, Geology and organic geochemistry of the Woodford Shale in the Criner Hills and western Arbuckle Mountains, Oklahoma, *in* Johnson, K., and Cardott, B.J., eds., Source Rocks in the southern midcontinent: Oklahoma Geological Survey, Circular 93, p. 38–69.

Kleehammer, R.S., 1991, Conodont biostratigraphy of Late Mississippian shale sequences, south-central Oklahoma [MS Thesis]: University of Oklahoma, Norman, 135 p.

Kluth, C.F., and Coney, P.J., 1981, Plate tectonics of the Ancestral Rocky Mountains: Geology, v. 9, p. 10–15.

Koffman, B.G., Yoder, M.F., Methven, T., Hanschka, L., Sears, H.B., Saylor, P.L., and Wallace, K.L., 2021, Glacial dust surpasses both volcanic ash and desert dust in its iron fertilization potential: Global Biogeochemical Cycles, v. 35, no. e2020GB006821.

Kondas, M., Filipiak, P., Paszkowski, M., Pisarzowska, A., Elmore, R.D., Jelonek, I., and Kasprzyk, M., 2018, The organic matter composition of the Devonian/Carboniferous deposits (South Flank of Arbuckle Anticline, Oklahoma, USA): International Journal of Coal Geology, v. 198, p. 88–99.

Konstantinou, A., Wirth, K.R., Vervoort, J.D., Malone, D.H., Davidson, C., and Craddock, J.P., 2014, Provenance of quartz arenites of the Early Paleozoic Midcontinent Region, USA: The Journal of Geology, v. 122, p. 201–216.

Kuuskraa, V.A., 2011, Worldwide assessment underscores vast potential of gas shale resources: American Oil & Gas Reporter, v. 54, p. 40–46.

Lakin, J.A., Marshall, J.E.A., Troth, I., and Harding, I.C., 2016, Greenhouse to icehouse: a biostratigraphic review of latest Devonian–Mississippian glaciations and their global effects, *in* Becker, R.T., Königshof, P., and Brett, C.E., eds., Devonian Climate, Sea Level and Evolutionary Events: Geological Society of London, Special Publication 423, p. 439–464.

Lane, H.R., and De Keyser, T.L., 1980, Paleogeography of the late Early Mississippian (Tournaisian 3) in the central and southwestern United States, *in* Fouch, T.D., and Magathan, E.R., eds., Paleozoic Paleogeography of the West-Central United States: SEPM, Rocky Mountain Section, p. 149–162.

Loucks, R.G., and Ruppel, S.C., 2007, Mississippian Barnett Shale: lithofacies and depositional setting of a deep-water shale-gas succession in the Fort Worth Basin, Texas: American Association of Petroleum Geologists, Bulletin, v. 9, p. 579–601.

Lowe, D.R., 1976, Nonglacial varves in lower member of Arkansas Novaculite (Devonian), Arkansas and Oklahoma: American Association of Petroleum Geologists, Bulletin, v. 60, p. 2103–2116.

Macquaker, J.H., Bentley, S.J., and Bohacs, K.M., 2010, Wave-enhanced sediment-gravity flows and mud dispersal across continental shelves: reappraising sediment transport processes operating in ancient mudstone successions: Geology, v. 38, p. 947–950.

Mankin, C.J., 1987, Texas–Oklahoma tectonic region, *in* Childs, O.E., Steele, G., Salvador, A., and Lindberg, F.A., eds., Correlation of Stratigraphic Units of North America: American Association of Petroleum Geologists, Correlation of Stratigraphic Units in North America, chart TOT.

Mazzullo, S.J., Boardman, D.R., Wilhite, B.W., Godwin, C., and Morris, B.T., 2013, Revisions of outcrop lithostratigraphic nomenclature in the Lower to Middle Mississippian Subsystem (Kinderhookian to basal Meramecian series) along the shelf-edge in southwest Missouri, northwest Arkansas, and northeast Oklahoma: Shale Shaker, v. 63, p. 414–454.

Mazzullo, S.J., Wilhite, B.W., Boardman, D.R., Morris, B.T., and Godwin, C.J., 2019, Lithostratigraphy, biostratigraphy, stratigraphic architecture, and depositional systems in Lower to Middle Mississippian strata on the western flank of the Ozark Dome, midcontinent U.S.A., *in* Grammer, G.M., Gregg, J.M., Puckette, J., Jaiswal, P., Mazzullo, S.J., Pranter, M.J., and Goldstien, R.H., eds., Mississippian Reseviors of the Midcontinent: American Association of Petroleum Geologists, Memoir 112, p. 25–58.

McGowan, H.A., Sturman, A.P., and Owens, I.F., 1996, Aeolian dust transport and deposition by foehn winds in an alpine environment, Lake Tekapo, New Zealand: Geomorphology, v. 15, p. 135–146.

Meert, J.G., and Torsvik, T.H., 2003, The making and unmaking of a supercontinent: Rodinia revisited: Tectonophysics, v. 375, p. 261–288.

Milad, B., Slatt, R., and Fuge, Z., 2020, Lithology, stratigraphy, chemostratigraphy, and depositional environment of the Mississippian Sycamore rock in the SCOOP and STACK area, Oklahoma, USA: field, lab, and machine learning studies on outcrops and subsurface wells: Marine and Petroleum Geology, v. 115, no. 104278.

Miller, J., and Cullen, A., 2018, My favorite outcrop: Sycamore Formation I-35 South, Arbuckle Mountains, OK: Shale Shaker, v. 69, p. 87–99.

Miller, J.C., Pranter, M.J., and Cullen, A.B., 2019a, Regional stratigraphy and organic richness of the Mississippian Meramec and associated strata, Anadarko Basin, central Oklahoma: Shale Shaker, v. 70, p. 50–79.

Miller, J.D., Puckette, J.O., and Godwin, C.J., 2019b, Conodont biostratigraphy constrained diachronous lithofacies, Boone Group (upper Osagean to lower Meramecian), Western Ozarks: breakdown of lithostratigraphic correlations at the regional scale, *in* Grammer, G.M., Gregg, J.M., Puckette, J.O., Jaiswal, P., Mazzullo, S.J., Pranter, M.J., and Goldstein, R.H., eds., Mississippian Reservoirs of the Midcontinent: American Association of Petroleum Geologists, Memoir 122, p. 89–106.

Miller, M.J., Pranter, M.J., Gupta, I., Devegowda, D., Marfurt, C., Sondergeld, C., Rai, C., McLain, C.T., Packwood, J., and Larese, R., 2021, Mississippian Meramec lithologies and petrophysical property variability, STACK trend, Anadarko Basin, Oklahoma: Interpretation, v. 9, SE1–SE21.

Muhs, D.R., Roskin, J., Tsoar, H., Skipp, G., Budahn, J.R., Sneh, A., Porat, N., Stanley, J.D., Katra, I., and Blumberg, D.G., 2013, Origin of the Sinai–Negev erg, Egypt and Israel: mineralogical and geochemical evidence for the importance of the Nile and sea level history: Quaternary Science Reviews, v. 69, p. 28–48.

Müller, R.D., Cannon, J., Qin, X., Watson, R.J., Gurnis, M., Williams, S., Pfaffelmoser, T., Seton, M., Russell, S.H., and Zahirovic, S., 2018, GPlates: building a virtual Earth through deep time: Geochemistry, Geophysics, Geosystems, v. 19, p. 2243–2261, doi:10.1029/2018GC007584.

Nance, R.D., Gutiérrez-Alonso, G., Keppie, J.D., Linnemann, U., Murphy, J.B., Quesada, C., Strachan, R.A., and Woodcock, N.H., 2010, Evolution of the rheic ocean: Gondwana Research, v. 17, p. 194–222, doi:10.1016/j.gr.2009.08.00.

Newell, D.H., Watney, L.W., Stephen, W.L., Cheng, S., and Brownrigg, R., 1987, Stratigraphic and Spatial Distribution of Oil and Gas Production in Kansas: Kansas Geological Survey, Subsurface Geology Series 9.

Norte, F.A., 2015, Understanding and forecasting Zonda wind (Andean Foehn) in Argentina: a review: Atmospheric and Climate Sciences, v. 5, p. 163–193.

Northcutt, R.A., Campbell, J.A., 1995, Geological provinces of Oklahoma: Oklahoma Geological Survey, Open-File Report 5-95, 1 sheet, scale 1:750,000, 6 page explanation and bibliography.

Oklahoma Corporation Commission, 2021, Well Completion List Master, https://oklahoma.gov/occ/divisions/oil-gas/oil-gas-data.html.

Over, D.J., 1990, Conodont biostratigraphy of the Woodford Shale (late Devonian–early Carboniferous) in the Arbuckle Mountains, south-central Oklahoma [Ph.D. Thesis]: Texas Tech University, Lubbock, 186 p.

Park, H., Barbeau, D.L., Jr., Rickenbaker, A., Bachmann-Krug, D., and Gehrels, G., 2010, Application of foreland basin detrital-zircon geochronology to the reconstruction of the southern and central Appalachian orogen: The Journal of Geology, v. 118, p. 23–44.

Patchen, D.G., Avary, K.L., and Erwin, R.B., 1984a, Southern Appalachians region *in* Childs, O.E., Steele, G., Salvador, A., and Lindberg, F.A., eds., Correlation of

Stratigraphic Units of North America: American Association of Petroleum Geologists, Correlation of Stratigraphic Units in North America, chart SAP.

Patchen, D.G., Avary, K.L., and Erwin, R.B., 1984b, Northern Appalachians Region, *in* Childs, O.E., Steele, G., Salvador, A., Lindberg, F.A., eds., Correlation of Stratigraphic Units of North America: American Association of Petroleum Geologists, Correlation of Stratigraphic Units in North America, chart NAP.

Perry, W.J., 1989, Tectonic evolution of the Anadarko basin region, Oklahoma: U.S. Geological Survey, Bulletin 1866, 19 p.

Price, B.J., Pollack, A.C., Lamb, A.P., Peryam, T.C., and Anderson, J.R., 2020, Depositional interpretation and sequence stratigraphic control on reservoir quality and distribution in the Meramecian Sooner trend Anadarko Basin, Canadian, and Kingfisher counties (STACK) play, Anadarko Basin, Oklahoma, United States: American Association of Petroleum Geologists, Bulletin, v. 104, p. 357–386.

Puliafito, S.E., Allende, D.G., Mulena, C.G., Cremades, P., and Lakkis, S.G., 2015, Evaluation of the WRF model configuration for Zonda wind events in a complex terrain: Atmospheric Research, v. 166, p. 24–32.

Pullen, A., Ibáñez-Mejia, M., Gehrels, G.E., Giesler, D., and Pecha, M., 2018, Optimization of a laser ablation-single collector-inductively coupled plasma-mass spectrometer (Thermo Element 2) for accurate, precise, and efficient zircon U-Th-Pb geochronology: Geochemistry, Geophysics, Geosystems, v. 19, p. 3689–3705, doi:10.1029/2018GC007889.

Rea, D.K., and Janecek, T.R., 1981, Late cretaceous history of eolian deposition in the mid-pacific mountains, central North Pacific Ocean: Palaeogeography, Palaeoclimatology, Palaeoecology, v. 36, p. 55–67.

Richardson, J.G., and Ausich, W.I., 2005, Miospore biostratigraphy of the Borden Delta (Lower Mississippian; Osagean) in Kentucky and Indiana, USA: Palynology v. 28, p. 159–174, doi:10.2113/28.1.159.

Rickard, W.D., Gluth, G.J., and Pistol, K., 2016, In-situ thermo-mechanical testing of fly ash geopolymer concretes made with quartz and expanded clay aggregates: Cement and Concrete Research, v. 80, p. 33–43.

Rimmer, S.M., 2004, Geochemical paleoredox indicators in Devonian–Mississippian black shales, Central Appalachian Basin (USA): Chemical Geology, v. 206, p. 373–391, doi:10.1016/j.chemgeo.2003.12.029.

Sandberg, C.A., and Gutschick, R.C., 1980, Sedimentation and biostratigraphy of Osagean and Meramecian starved basin and foreslope, western United States, *in* Fouch, T.D., and Magathan, E.R., eds., Paleozoic Paleogeography of the West-Central United States: SEPM, Rocky Mountain Section, p. 129–147.

Schieber, J., 2016, Mud re-distribution in epicontinental basins: exploring likely processes: Marine and Petroleum Geology, v. 71, p. 119–133.

Schomburg, J., 1991, Thermal reactions of clay minerals: their significance as "archaeological thermometers" in ancient potteries: Applied Clay Science, v. 6, p. 215–220.

Scotese, C.R., and Wright, N., 2018, PALEOMAP Paleodigital Elevation Models (PaleoDEMS) for the Phanerozoic: https://www.earthbyte.org/paleodem-resource-scotese-and-wright-2018/.

Schwartzapfel, J.A., 1990, Biostratigraphic investigations of Late Paleozoic (Upper Devonian to Mississippian) radiolaria within the Arbuckle Mountains and Ardmore Basin of south-central Oklahoma [Ph.D. Thesis]: University of Texas at Dallas, 475 p.

Schwartzapfel, J.A., and Holdsworth, B.K., 1996, Upper Devonian and Mississippian radiolarian zonation and biostratigraphy of the Woodford, Sycamore, Caney and Goddard formations, Oklahoma: Cushman Foundation for Foraminiferal Research, Special Publication 33, p. 1–275.

Sevon, W.D., 1985, Nonmarine facies of the Middle and Late Devonian Catskill coastal alluvial plain, *in* Woodrow, D.L., and Sevon, W.D., eds., The Catskill Delta: Geological Society of America, Special Paper 201, p. 79–90.

Shaver, R.H., 1985, Midwest basin and arches region, *in* Childs, O.E., Steele, G., Salvador, A., and Lindberg, F.A., eds., Correlation of Stratigraphic Units of North America: American Association of Petroleum Geologists, Correlation of Stratigraphic Units in North America, chart MBA.

Shelley, S., Grammer, G.M., and Pranter, M.J., 2019, Outcrop-based reservoir characterization and modeling of an Upper Mississippian mixed carbonate–siliciclastic ramp, northeastern Oklahoma, *in* Grammer, G.M., Gregg, J.M., Puckette, J.O., Jaiswal, P., Mazzullo, S.J., Pranter, M.J., and Goldstein, R.H., eds., Mississippian Reservoirs of the Midcontinent: American Association of Petroleum Geologists, Memoir 122, p. 207–226.

Slatt, R.M., and O'Brien, N.R., 2011, Pore types in the Barnett and Woodford gas shales: contribution to understanding gas storage and migration pathways in fine-grained rocks: American Association of Petroleum Geologists, Bulletin, v. 95, p. 2017–2030.

Smith, M.G., and Bustin, R.M., 1998, Production and preservation of organic matter during deposition of the Bakken Formation (Late Devonian and Early Mississippian), Williston Basin: Palaeogeography, Palaeoclimatology, Palaeoecology, v. 142, p. 185–200.

Smith, M.G., and Bustin, R.M., 2000, Late Devonian and Early Mississippian Bakken and Exshaw black shale source rocks, Western Canada Sedimentary Basin: a sequence stratigraphic interpretation: American Association of Petroleum Geologists, Bulletin v. 84, p. 940–960.

Soeder, D.J., Enomoto, C.B., and Chermak, J.A., 2014, The Devonian Marcellus Shale and Millboro Shale, *in* Bailey, C.M., and Coiner, L.V., eds., Elevating Goescience in the Southeastern United States: New Ideas about Old Terranes: Geological Society of America, Field Guide 35, p. 129–160.

Sonnenberg, S.A., 2011, TOC and pyrolysis dada for the Bakken Formation, Williston Basin: Bulletin of Canadian Petroleum Geology, v. 44, p. 495–507.

Soreghan, G.S., 1992, Preservation and paleoclimatic significance of eolian dust in the Ancestral Rocky Mountains province: Geology, v. 20, p. 1111–1114.

Soreghan, M.J., and Soreghan, G.S., 2007, Whole-rock geochemistry of upper Paleozoic loessite, western Pangaea: implications for paleo-atmospheric circulation: Earth and Planetary Science Letters, v. 255, p. 117–132.

Soreghan, G.S., Soreghan, M.J., and Hamilton, M.A., 2008, Origin and significance of loess in late Paleozoic western Pangaea: a record of tropical cold?: Palaeogeography, Palaeoclimatology, Palaeoecology, v. 268, p. 234–259.

Soreghan, G.S., Soreghan, M.J., and Heavens, N.G., 2019, Explosive volcanism as a key driver of the late Paleozoic ice age: Geology, v. 47, p. 600–604.

Stevens, J., 2017a, Connecting the dots between dust, phytoplankton, and ice cores: NASA, Image of the Day, November 15, 2017, https://earthobservatory.nasa.gov/images/91267/connecting-the-dots-between-dust-phytoplankton-and-ice-cores.

Stevens, J., 2017b, Dust coats Copper River Valley: NASA, Image of the Day, November 19, 2017, https://earthobservatory.nasa.gov/images/91303/dust-coats-copper-river-valley.

Stow, D.A.V., Huc, A.Y., and Bertrand, P., 2001, Depositional processes of black shale in deep water: Marine and Petroleum Geology, v. 18, p. 491–498.

Sur, S., Soreghan, M.J., Soreghan, G.S., and Stagner, A.F., 2010a, Extracting the silicate mineral fraction from ancient carbonate: assessing the geologic record of dust: Journal of Sedimentary Research, v. 80, p. 763–769.

Sur, S., Soreghan, G.S., Soreghan, M.J., Yang, W., and Saller, A.H., 2010b, A record of glacial aridity and Milankovitch-scale fluctuations in atmospheric dust from the Pennsylvanian tropics: Journal of Sedimentary Research, v. 80, p. 1046–1067.

Sur, S., Owens, J.D., Soreghan, G.S., Lyons, T.W., Raiswell, R., Heavens, N.G., and Mahowald, N.M., 2015, Extreme eolian delivery of reactive iron to late Paleozoic icehouse seas: Geology, v. 43, p. 1099–1102.

Sweet, A.C., Soreghan, G.S., Sweet, D.E., Soreghan, M.J., and Madden, A.S., 2013, Permian dust in Oklahoma: source and origin for middle Permian (Flowerpot–Blaine) redbeds in western tropical Pangaea: Sedimentary Geology, v. 284, p. 181–196.

Swet, N., Elperin, T., Kok, J.F., Martin, R.L., Yizhaq, H., and Katra, I., 2019, Can active sands generate dust particles by wind-induced processes?: Earth and Planetary Science Letters, v. 506, p. 371–380.

Swet, N., Kok, J.F., Huang, Y., Yizhaq, H., and Katra, I., 2020, Low dust generation potential from active sand grains by wind abrasion: Journal of Geophysical Research, Earth Surface, v. 125, no. e2020JF005545.

Taylor, S.R., and McLennan, S.M., 1985, The Continental Crust: Its Composition and Evolution: an Examination of the Geochemical Record Preserved in Sedimentary Rocks, Blackwell Scientific Publishing, 1985, 312 p.

Taylor, S.R., McLennan, S.M., and McCulloch, M.T., 1983, Geochemistry of loess, continental crustal composition and crustal modal ages: Geochimica et Cosmochimica Acta, v. 47, p. 1897–1905.

Thomas, W.A., Becker, T.P., Samson, S.D., and Hamilton, M.A., 2004, Detrital zircon evidence of a recycled orogenic foreland provenance for Alleghanian clastic-wedge sandstones: The Journal of Geology, v. 112, p. 23–37.

Thomas, W.A., Gehrels, G.E., Greb, S.F., Nadon, G.C., Satkoski, A.M., and Romero, M.C., 2017, Detrital Zircons and sediment dispersal in the Appalachian foreland: Geosphere, v. 13, p. 2206–2230.

Thomas, W.A., Gehrels, G.E., Sundell, K.E., Greb, S.F., Finzel, E.S., Clark, R.J., Malone, D.H., Hampton, B.A., and Romero, M.C., 2020, Detrital zircons and sediment dispersal in the eastern Midcontinent of North America: Geosphere, v. 16, p. 817–843.

Turner, B.W., Molinares-Blanco, C.E., and Slatt, R.M., 2015, Chemostratigraphic, palynostratigraphic, and sequence stratigraphic analysis of the Woodford Shale, Wyche Farm Quarry, Pontotoc County, Oklahoma: Interpretation, v. 3, SH1–SH9.

Turner, B.W., Tréanton, J.A., and Slatt, R.M., 2016, The use of chemostratigraphy to refine ambiguous sequence stratigraphic correlations in marine mudrocks. An example from the Woodford Shale, Oklahoma, USA: Geological Society of London, Journal, v. 173, p. 854–868.

Ulmishek, G.F., and Klemme, H.D., 1990, Depositional controls, distribution, and effectiveness of world's petroleum source rocks: U.S. Geological Survey, Bulletin 1931, 59 p.

Valdes, P.J., Armstrong, E., Badger, M.P., Bradshaw, C.D., Bragg, F., Crucifix, M., Davies-Barnard, T., Day, J.J., Farnsworth, A., Gordon, C., and Hopcroft, P.O., 2017, The BRIDGE HadCM3 family of climate models: HadCM3@ Bristol v1. 0: Geoscientific Model Development, v. 10, p. 3715–3743.

Valdes, P.J., Scotese, C.R., and Lunt, D.J., 2021, Deep ocean temperatures through time: Climate of the Past, v. 17, p. 1483–1506.

Van Schmus, W.R., Bickford, M.E., Anderson, J.F., Bender, E.E., Anderson, R.R., Bauer, P.W., Robertson, J.M., Bowring, S.A., Condie, K.C., Denison, R.E., Gilbert, M.C., Grambling, J.A., Mawer, C.K., Shearer, C.K., Hinze, W.J., Karlstrom, K.E., Kisvarsanyi, E.B., Lidiak, E.G., Reed, J.C., Sims, P.K., Tweto, O., Silver, L.T., Treves, S.B., Williams, M.L., and Wooden, J.L., 1993, Transcontinental Proterozoic provinces, *in* Reed, J.C., Jr., Sims, P.K., Houston, R.S., Silver, L.T., Rankin, D.W., and Reynolds, M.W., eds., Precambrian: Conterminous US: Geological Society of America, the Geology of North America v. C-2, p. 171–334.

Walsh, J.P., and Nittrouer, C.A., 2009, Understanding fine-grained river-sediment dispersal on continetal margins: Marine Geology, v. 263, p. 34–45.

Wang, T., and Philp, R.P., 2019, Oil families and inferred source rocks of the Woodford–Mississippian tight oil play in northcentral Oklahoma: American Association of Petroleum Geologists, Bulletin, v. 103, p. 871–903.

Washington, R., Todd, M.C., Lizcano, G., Tegen, I., Flamant, C., Koren, I., Ginoux, P., Engelstaedter, S., Bristow, C.C., Zender, C.S., Goudie, A.S., Warren, A., and Prospero, J.M., 2006, Links between topography, wind, deflation, lakes and dust: the case of the Bodélé Depression, Chad: Geophysical Research Letters, v. 33, no. L09401

Whitmeyer, S.J., and Karlstrom, K.E., 2007, Tectonic model for the Proterozoic growth of North America: Geosphere, v. 3, p. 220–259.

Wickham, J., 1978, The southern Oklahoma Alucogen, in structural style of the Arbuckle region: Geological Society of America, South-Central Section, Field Trip 3, p. 8–41.

Woodrow, D.L., 1985, Paleogeography, paleoclimate, and sedimentary processes of the Late Devonian Catskill Delta, *in* Woodrow, D.L., and Sevon, W.D., eds., The Catskill Delta: Geological Society of America, Special Paper 201, p. 51–63.

Wright, L.D., and Friedrichs, C.T., 2006, Gravity-driven sediment transport on continental shelves: a status report: Continental Shelf Research, v. 26, p. 2092–2107.

Wynn, T.C., and Read, J.F., 2008, Three-dimensional sequence analysis of a subsurface carbonate ramp, Mississippian Appalachian foreland basin, West Virginia, USA: Sedimentology, v. 55, p. 357–394.

Zou, Y., and Xi, X., 2021, An ongoing cooling in the eastern Pacific linked to eastward migration of the Southeast Pacific Subtropical Anticyclone: Environmental Research Letters, v. 16, no. 034020.

Received 1 February 2022; accepted 20 September 2022.